



1 **Exploring the impacts of unprecedented climate extremes on forest ecosystems: hypotheses**
2 **to guide modeling and experimental studies**

3

4 Jennifer A. Holm^{1,*}, David M. Medvigy², Benjamin Smith^{3,4}, Jeffrey S. Dukes⁵, Claus Beier⁶,
5 Mikhail Mishurov³, Xiangtao Xu⁷, Jeremy W. Lichstein⁸, Craig D. Allen⁹, Klaus S. Larsen⁶, Yiqi
6 Luo¹⁰, Cari Ficken¹¹, William T. Pockman¹², William R.L. Anderegg¹³, and Anja Rammig¹⁴

7

8 ¹ Lawrence Berkeley National Laboratory, Berkeley, California, USA

9 ² University of Notre Dame, Notre Dame, Indiana, USA

10 ³ Dept of Physical Geography and Ecosystem Science, Lund University, Lund, Sweden

11 ⁴ Hawkesbury Institute for the Environment, Western Sydney University, Penrith, NSW 2751,
12 Australia

13 ⁵ Department of Forestry and Natural Resources and Biological Sciences, Purdue University,
14 West Lafayette, Indiana, USA

15 ⁶ Department of Geosciences and Natural Resource Management, University of Copenhagen,
16 Frederiksberg, Denmark

17 ⁷ Department of Ecology and Evolutionary Biology, Cornell University, Ithaca, New York, USA

18 ⁸ Department of Biology, University of Florida, Gainesville, Florida, USA

19 ⁹ U.S. Geological Survey, Fort Collins Science Center, New Mexico Landscapes Field Station,
20 Los Alamos, New Mexico, USA

21 ¹⁰ Center for Ecosystem Science and Society, Department of Biological Sciences, Northern
22 Arizona University, Flagstaff, Arizona, USA

23 ¹¹ Department of Biology, University of Waterloo, Waterloo, Ontario, Canada

24 ¹² Department of Biology, University of New Mexico, Albuquerque, New Mexico, USA

25 ¹³ School of Biological Sciences, University of Utah, Salt Lake City, Utah, USA

26 ¹⁴ Technical University of Munich, TUM School of Life Sciences Weihenstephan, Freising,
27 Germany

28

29 * *Correspondence to:* Jennifer Holm; 510-495-8083; jaholm@lbl.gov

30

31 **Keywords:** demographic modeling; mortality; drought; recovery; carbon cycle; nonstructural
32 carbohydrate storage; plant hydraulics; dynamic vegetation

33



34 **Abstract**

35

36 Climatic extreme events are expected to occur more frequently in the future, increasing the
37 likelihood of unprecedented climate extremes (UCEs), or record-breaking events. UCEs, such as
38 extreme heatwaves and droughts, substantially affect ecosystem stability and carbon cycling by
39 increasing plant mortality and delaying ecosystem recovery. Quantitative knowledge of such
40 effects is limited due to the paucity of experiments focusing on extreme climatic events beyond
41 the range of historical experience. Here, we use two dynamic vegetation demographic models
42 (VDMs), ED2 and LPJ-GUESS, to investigate the hypothesis that ecosystem responses to UCEs
43 (e.g., unprecedented droughts) differ qualitatively from ecosystem responses to milder extremes,
44 as a result of non-linear ecosystem responses. Additionally, we explore how unprecedented
45 droughts in combination with increasing atmospheric CO₂ and/or temperature may affect
46 ecosystem stability and carbon cycling. We explored these questions using simulations of pre-
47 drought and post-drought conditions at well-studied forest sites in Australia and Costa Rica. Both
48 models produced nonlinear responses to UCEs. Due to the two models having different but
49 plausible representations of processes and interactions, they diverge in sensitivity of biomass loss
50 due to drought duration or intensity, and differ between each site. Biomass losses are most
51 sensitive to drought duration in ED2, but to drought intensity in LPJ-GUESS. Elevated
52 atmospheric CO₂ concentrations (eCO₂) alone did not completely buffer the ecosystems from
53 carbon losses during UCEs in the majority of our simulations. Our findings highlight contrasting
54 differences in process formulations and uncertainties in models, notably related to availability in
55 plant carbohydrate storage and the diversity of plant hydraulic schemes, in projecting potential
56 ecosystem responses to UCEs. The different hypotheses of plant responses to UCEs existing in
57 models reflect knowledge gaps, which should be tested with targeted field experiments. This
58 iterative modeling-experimental framework would help improve predictions of terrestrial
59 ecosystem responses and climate feedbacks.



60 **1 Introduction**

61 The increase in extreme climate and weather events, such as prolonged heatwaves and
62 droughts as seen over the last three decades, are expected to continue to increase in frequency
63 and magnitude, leading to progressively longer and warmer droughts on land (IPCC 2012, 2021).
64 Droughts are affecting all areas of the globe, more than any other natural disturbance, and recent
65 droughts have broken long-standing records (Ciais et al., 2005; Phillips et al., 2009; Williams et
66 al., 2012; Matusick et al., 2013; Griffin and Anchukaitis, 2014; Asner et al., 2016; Feldpausch et
67 al., 2016; Seneviratne et al., 2021). Such ‘unprecedented climate extremes’ (UCEs; “record-
68 breaking events”, IPCC (2012)) that are larger in extent and longer-lasting than historical norms
69 can have dramatic consequences for terrestrial ecosystem processes, including carbon uptake and
70 storage and other ecosystem services (Reichstein et al., 2013; Settele, 2014; Allen et al., 2015;
71 Brando et al., 2019; Kannenberg et al., 2020). Thus, to better anticipate the implications of
72 climatic changes for the terrestrial carbon sink and other ecosystem services, we need to better
73 understand how ecosystems respond to extreme droughts and other UCEs.

74 To learn how ecosystems respond to rarely experienced or unprecedented conditions,
75 ecologists can experimentally manipulate environmental conditions (Rustad, 2008; Beier et al.,
76 2012; Meir et al., 2015; Aguirre et al., 2021). However, the majority of such experiments apply
77 moderate treatments, which are mostly weaker in intensity and/or shorter in duration than
78 potential future UCEs (Beier et al., 2012; Kayler et al., 2015; but see Luo et al., 2017), and single
79 experiments have low power to detect effects of stressors on ecosystem responses (Yang et al.,
80 2022). Additionally, most experiments examine low-stature ecosystems, such as grassland,
81 shrubland or tundra, due to lower requirements for infrastructure and financial investment
82 compared to mature forests. However, forests may respond qualitatively differently to UCEs than
83 other ecosystems, in part due to mortality of large trees and strong nonlinear ecosystem
84 responses, with long-lasting consequences for ecosystem-climate feedbacks (Williams et al.,
85 2014; Meir et al., 2015). Ecosystem responses to naturally occurring extreme droughts and
86 heatwaves have been documented (Ciais et al., 2005; Breshears et al., 2009; Feldpausch et al.,
87 2016; Matusick et al., 2016; Ruthrof et al., 2018; Powers et al., 2020); however, these rapidly-
88 mobilized post-hoc studies often are unable to measure all critical variables and may lack
89 consistently collected data for comparison with pre-drought conditions, thus limiting their
90 inferential power and ability to improve quantitative models. The difficulties of performing



91 controlled real-world experiments of UCEs at broad spatial and temporal scales make process-
92 based modeling a valuable tool for studying potential ecosystem responses to extreme events.
93 Process-based models can be used to explore potential ecosystem impacts using projected
94 climate change over broad spatial and temporal scales (Gerten et al., 2008; Luo et al., 2008;
95 Zscheischler et al., 2014; Sippel et al., 2016), as seen in a few modeling studies that have
96 synthesized and improved our process-level understanding of UCE effects (McDowell et al.,
97 2013; Dietze and Matthes, 2014). However, due to the overly simplified representation of
98 ecological processes in most land surface models (LSMs) – the terrestrial components of Earth
99 System Models (ESMs) used for climate projections – it is doubtful whether most of these
100 models adequately capture ecosystem feedbacks and other responses to UCEs (Fisher and
101 Koven, 2020). For example, only a few ESMs in recent coupled model intercomparison projects
102 (CMIP6) and IPCC climate assessments (Ciais et al., 2013; Arora et al., 2020) include vegetation
103 demographics (Döscher et al., 2022), and most rely on prescribed, static maps of plant functional
104 types (PFTs) (Ahlström et al., 2012). Other LSMs simulate PFT shifts (i.e., dynamic global
105 vegetation models, DGVMs; Sitch et al., (2008)) based on bioclimatic limits, instead of
106 emerging from the physiology- and competition-based demographic rates that determine
107 resource competition and plant distributions in real ecosystems (Fisher et al., 2018). Although a
108 new generation of LSMs with more explicit ecological dynamics and structured demography is
109 emerging (Holm et al., 2020; Koven et al., 2020; Döscher et al., 2022), most current ESMs are
110 limited in ecological detail and realism (e.g., ecosystem structure, demography, and
111 disturbances). Failing to mechanistically represent mortality, recruitment, and disturbance – each
112 of which influences biomass turnover and carbon (C) allocation (Friend et al., 2014) – limits the
113 ability of these models to realistically forecast ecosystem responses to anomalous environmental
114 conditions like UCEs (Fisher et al., 2018).

115 Evaluating and improving the representation of physiological and ecological processes in
116 ecosystem models is critical for reducing model uncertainties when projecting the effects of
117 UCEs on long-term ecosystem dynamics and functioning (Table 1). Vegetation demography,
118 plant hydraulics, enhanced representations of plant trait variation, explicit treatments of resource
119 competition (e.g., height-structured competition for light), and representing major disturbances
120 (e.g., extreme drought) have all been identified as critical areas for advancing current models
121 (Scheiter et al., 2013; Fisher et al., 2015; Weng et al., 2015; Choat et al., 2018; Fisher et al.,



122 2018) and are necessary advances for realistically representing the ecosystem impacts of UCEs.
123 Uncertainty in these processes leads to uncertainty in predicting an ecosystem's pre-drought
124 resistance, which influences the degree of impact and recovery from UCEs (Table 1; Frank et al.,
125 (2015)).

126 In this paper, we explore the potential responses of forest ecosystems to UCEs using two
127 state-of-the-art process-based demographic models (vegetation demographic models, VDMs;
128 Fisher et al., (2018)). We first present conceptual frameworks and hypotheses on potential
129 ecosystem responses to UCEs based on current knowledge. We then present VDM simulations
130 for a range of hypothetical UCE scenarios to illustrate current state-of-the-art model
131 representations of eco-physiological mechanisms expected to drive responses to UCEs. While a
132 variety of UCE-linked biophysical tree disturbance processes (e.g., fire, wind, insect outbreaks)
133 can drive non-linear ecosystem responses, we focus specifically on extreme droughts, which
134 have important impacts on many ecosystems around the world (e.g. Frank et al., 2015, IPCC
135 2021). By studying modeled responses to UCEs, we explore the limits to our current
136 understanding of ecosystem responses to extreme droughts and their corresponding thresholds
137 and tipping points. As anthropogenic forcing has increased the frequency, duration, and intensity
138 of droughts throughout the world (Chiang et al., 2021), we explore how eCO₂ and rising
139 temperatures may affect drought-induced C loss and recovery trajectories, and how the scientific
140 community can iteratively address these questions through experiments and modeling studies.

141

142 **1.1 Conceptual and Analysis Framework for Hypothesis Testing:**

143 This section presents conceptual frameworks that allow us to test two hypotheses on
144 potential responses of plant carbon stocks to UCEs. The first hypothesis is:

145 ***Hypothesis (H1). Terrestrial ecosystem responses to UCEs will differ qualitatively from***
146 ***ecosystem responses to milder extremes because responses are nonlinear. Nonlinearities can***
147 ***arise from multiple mechanisms – including shifts in plant hydraulics, C allocation,***
148 ***phenology, and stand demography – and can vary depending on the pre-drought state of the***
149 ***ecosystem.***

150 We present four conceptual relationships that describe terrestrial ecosystem responses to varying
151 degrees of extreme events (Fig. 1). Change in vegetation C stock is *linearly* related to drought



152 intensity and/or drought duration (Fig. 1a, H0, null hypothesis), which has some observational
153 support from annual and perennial grassland ecosystems, shrublands and savannas across the
154 globe (Bai et al., 2008; Muldavin et al., 2008; Ruppert et al., 2015). Alternatives to the null
155 (linear) hypothesis are that biomass loss increases non-linearly with increased drought intensity
156 (i.e., reduction in precipitation) represented by a threshold-based relationship (Fig. 1a, H1a),
157 increased drought duration (i.e., prolonged drought with the same intensity) by shifting the linear
158 relationship downwards via increasing slopes (Fig. 1a, H1b), or the combination of both intensity
159 and duration (Fig. 1a, H1c). These hypotheses are supported by observations from the Amazon
160 Basin and Borneo (Phillips et al., 2010) where tree mortality rates increased non-linearly with
161 drought intensity. Similarly, plant hydraulic theories predict nonlinear damage to the plant-water
162 transport systems, and thus mortality risk, as a function of drought stress (Sperry and Love,
163 2015). In particular, longer droughts are more likely to lead to lower soil water potentials,
164 leading to a nonlinear xylem damage function even if stomata effectively limit water loss (Sperry
165 et al., 2016).

166 ***Hypothesis (H2): The effects of increasing atmospheric CO₂ concentration (eCO₂) will***
167 ***alleviate impacts of extreme drought stress through an increase in vegetation productivity and***
168 ***water-use efficiency, but only up to a threshold of drought severity, while increased***
169 ***temperature (and related water stress) will exacerbate tree mortality.***

170 This second hypothesis is based on growing evidence that effects of eCO₂ and climate
171 warming may interact with effects of drought intensity on ecosystems. The CO₂ fertilization
172 effect enhances vegetation productivity (e.g., net primary production, NPP) (Ainsworth and
173 Long, 2005; Norby et al., 2005; Wang et al., 2012), but this fertilization effect is generally
174 reduced by drought (Hovenden et al., 2014; Reich et al., 2014; Gray et al., 2016). Drought events
175 often coincide with increased temperature, which intensifies the impact of drought on
176 ecosystems (Allen et al., 2015; Liu et al., 2017), resulting in nonlinear responses in mortality
177 rates (Adams et al., 2009; Adams et al., 2017a). The evaluation of C cycling in VDMs with
178 doubling of CO₂ (only “beta effect”) showed a large carbon sink in a tropical forest (Holm et al.,
179 2020), but the inclusion of climate interactions in VDMs needs to be further explored.

180 Here, we relate ecosystem responses to UCEs by calculating the “integrated carbon (C)
181 loss” (Fig. 1b and see Methods), which integrates C loss from the beginning of the drought until



182 the time when C stocks have recovered to 50% of the pre-drought level. In response to drought,
183 warming, and eCO₂, divergent potential C responses (gains and losses; Fig. 1c) can be expected
184 (Keenan et al., 2013; Zhu et al., 2016; Adams et al., 2017a). For example, a grassland
185 macrocosm experiment found that eCO₂ completely compensated for the negative impact of
186 extreme drought on net carbon uptake due to increased root growth and plant nitrogen uptake,
187 and led to enhanced post-drought recovery (Roy et al., 2016). However, a 16-year grassland
188 FACE and the SoyFACE experiments showed that CO₂ fertilization effects were reduced or
189 eliminated under hotter/drier conditions (Gray et al., 2016; Obermeier et al., 2016). Reich et al.,
190 (2014) also found that CO₂ fertilization effects were reduced in a perennial grassland by water
191 and nitrogen limitation.

192 A corollary to our H2 is that conditions that favor productivity (e.g., longer growing
193 seasons and/or CO₂ fertilization) will enhance vegetation growth leading to “structural
194 overshoot” (SO; Fig. 1d; adapted from and supported by Jump et al., 2017), and can amplify the
195 effects of UCEs. Enhanced vegetation growth coupled with environmental variability can lead to
196 exceptionally high plant-water-demand during extreme drought and water stress, resulting in a
197 “mortality overshoot” (MO; Fig 1d). We conceptualize how oscillations between SO and
198 associated MO could be amplified by increasing climatic variability and UCEs (Fig. 1d).
199 Confidence is low as to how historically unprecedented eCO₂ levels and temperatures will affect
200 ecosystems in the future (i.e., the widening of the shaded areas compared to historical, Fig. 1d).
201 We expect, however that a rapidly changing climate, combined with effects of UCEs as a result
202 of more frequent extreme drought/heat events and drought stress, can exacerbate and amplify
203 SOs and MOs (Jump et al., 2017), leading to increasing C loss, even though various buffering
204 mechanisms exist (cf. (Lloret et al., 2012; Allen et al., 2015)). Relative to our conceptual (Fig.
205 1d), we note that most experimental, observational and modeling studies (Ciais et al., 2005; da
206 Costa et al., 2010; Phillips et al., 2010; Meir et al., 2015) take into account only low to moderate
207 drought intensities or single events, or combine drought with moderate effects of temperature
208 change. As represented by the increasing amplitude of oscillations in Fig. 1d, the interactions
209 between increased temperatures, UCE events, and vegetation feedbacks make ecosystem states
210 become inherently unpredictable, particularly over longer time-scales.

211



212 **2 Methods**

213 We explored our hypotheses at forested ecosystems in Australia and Central America
214 using two VDMs: the Lund-Potsdam-Jena General Ecosystem Simulator (LPJ-GUESS) (Smith et
215 al., 2001; Smith et al., 2014) and the Ecosystem Demography model 2 (ED2) (Medvigy et al.,
216 2009; Medvigy and Moorcroft, 2012). These models include detailed process representation of
217 ecosystem demography and dynamic plant growth, recruitment, and mortality, resulting in
218 changes in abundance of different PFTs, as well as vertically stratified tree size- and age-class
219 structure. Community dynamics and age-/size-structure are emergent properties from
220 competition for light, space, water, and nutrients, which dynamically and explicitly scale up from
221 the tree, to stand, to ecosystem level.

222 VDMs have been used to interpret the cascade of ecosystem responses to long-term
223 droughts in the Amazon and are informative when conducting model-data comparisons (Powell
224 et al., 2013), but studies of ecosystem responses to UCEs are lacking. New implementation of
225 plant competition for resources and plant hydraulics in VDMs are improving our understanding
226 of plant-water relations and stresses within plants (Christoffersen et al., 2016; Xu et al., 2016;
227 Fisher et al., 2018; and see Kennedy et al., 2019 for representation in a 'big-leaf' model). Since
228 field data needed to evaluate UCE responses are, by definition, unavailable, we do not perform
229 model-data comparisons. Rather, we use the model results to explore our hypotheses and
230 illustrate their implications for ecosystem responses under UCEs.

231

232 **2.1 LPJ-GUESS and ED2 Model Descriptions**

233 Both LPJ-GUESS and ED2 resolve vegetation into tree cohorts characterized by their
234 PFT, in addition to age-class in LPJ-GUESS; and size, and stem number density in ED2. Both
235 models are driven by external environmental drivers (e.g., temperature, precipitation, solar
236 radiation, atmospheric CO₂ concentration, nitrogen deposition), and soil properties (soil texture,
237 depth, etc.), and also depend on dynamic ecosystem state, which includes light attenuation, soil
238 moisture, and soil nutrient availability. Establishment and growth of PFTs, and their carbon-,
239 nitrogen- and water-cycles, are simulated across multiple patches per grid cell to account for
240 landscape heterogeneity. Both models characterize PFTs by physiological and bioclimatic
241 parameters, which vary between the models (Smith et al., 2001; Smith et al., 2014; Medvigy et
242 al., 2009; Medvigy and Moorcroft, 2012).



243 The LPJ-GUESS includes three woody PFTs: evergreen, intermediate evergreen, and
244 deciduous PFTs. Mortality in LPJ-GUESS is governed by a ‘growth-efficiency’-based function
245 ($\text{kg C m}^{-2} \text{ leaf yr}^{-1}$), which captures effects of water deficit, shading, heat stress, and tree size on
246 plant productivity relative to its resource-uptake capacity (leaf area), with a threshold below
247 which stress-related mortality risk increases markedly, in addition to background senescence and
248 exogenous disturbances. Stress mortality can be reduced by plants using labile carbon storage,
249 modeled implicitly using a ‘C debt’ approach, which buffers low productivity, enhancing
250 resilience to milder extremes (more details are given in section 4.1.4). Total mortality can thus be
251 impacted by variation in environmental conditions such as water limitation, low light conditions,
252 and nutrient constraints, as well as current stand structure (Smith et al., 2001; Hickler et al.,
253 2004).

254 The ED2 version used here (Xu et al., 2016) includes four woody PFTs: evergreen,
255 intermediate evergreen, deciduous, brevi-deciduous, and deciduous stem-succulent. This ED2
256 version includes coupled photosynthesis, plant hydraulics, and soil hydraulic modules (Xu et al.,
257 2016), which together determine plant water stress. The plant hydraulics module tracks water
258 flow along a soil–plant–atmosphere continuum, connecting leaf water potential, stem sap flow,
259 and transpiration, thus influencing controls on photosynthetic capacity, stomatal closure,
260 phenology, and mortality. Leaf water potential depends on time-varying environmental
261 conditions as well as time-invariant PFT traits. Leaf shedding is triggered when leaf water
262 potential falls below the turgor loss point (a PFT trait) for a sufficient amount of time. Leaf
263 flushing occurs when stem water potential remains high (above half of the turgor loss point) for a
264 sufficient time (see Xu et al., 2016 for details). PFTs differ in their hydraulic traits, wood
265 density, specific leaf area, allometries, rooting depth, and other traits. Stress-based mortality in
266 the ED2 version used here includes two main physiological pathways in our current
267 understanding of drought mortality (McDowell et al., 2013): C starvation and hydraulic failure.
268 Mortality due to C starvation in ED2 results from a reduction of C storage, a proxy for non-
269 structural carbohydrate (NSC) storage, which integrates the balance of photosynthetic gain and
270 maintenance cost under different levels of light and moisture availability. Mortality due to
271 hydraulic failure in ED2 is based on the percentage loss of stem conductivity. ED2 also includes
272 a density-independent senescence mortality rate based on wood density.



273 2.2 Modeling protocol

274 We applied LPJ-GUESS and ED2 at two extensively studied field sites. The first is a
275 mature *Eucalyptus* (*E. tereticornis*) warm temperate-subtropical transitional forest that is the site
276 of the Eucalyptus Free Air CO₂ enrichment (EucFACE) experiment in Western Sydney,
277 Australia (Medlyn et al., 2016; Ellsworth et al., 2017; Jiang et al., 2020), with a canopy coverage
278 of 95% (830 trees per ha). The EucFACE site has a mean annual temperature of 17.3°C and
279 receives an annual rainfall of 800 mm (Ellsworth et al., 2017). The evergreen eucalypt trees are
280 on average 22 m tall with a DBH of 21 cm and a stand-level LAI of 1.5. The second site is a
281 seasonally dry tropical forest in the Parque Nacional Palo Verde in Costa Rica (Powers et al.,
282 2009). This site has nutrient rich soils (Powers and Pérez-Aviles, 2013), a mean annual
283 temperature of 25.1°C, and mean annual rainfall of 1440 mm, with a 5-month dry season.
284 Multiple leaf phenological strategies co-occur, including evergreens, brevi-deciduous tree
285 species, as well as deciduous species that drop their leaves during the dry season.

286 We performed a 100-year “baseline” simulation for each model at each site driven by
287 constant, near ambient, atmospheric CO₂ (400 ppm) and recycled historical site-specific climate
288 data (1992-2011 for EucFACE and 1970-2012 for Palo Verde; Sheffield et al., (2006)), absent of
289 drought treatments. A detailed description of the meteorological data and initial conditions used
290 to drive the models is in the Supplementary Text A. No site-level parameter tuning was
291 conducted with the models. To describe the ecosystem impact of UCEs, we simulated 10 years
292 of pre-drought conditions (continuing from the baseline simulation), followed by drought
293 treatments that differed in intensity and duration, followed by a 100-year post-drought recovery
294 period. To explore the effects of drought intensity, we conducted 20 different artificial drought
295 intensity simulations, in which precipitation during the whole year is reduced by 5% to 100% of
296 its original amount, in increments of 5%. To explore the effects of drought duration, the 20
297 different drought intensities are maintained over 1, 2 and 4 years (Table S1). We examined
298 model responses of aboveground biomass, leaf area index (LAI), stem density (number ha⁻¹),
299 plant available soil water (mm), plant C storage (kg C m⁻²), change in stem mortality rate (yr⁻¹),
300 and PFT composition.

301 To explore how temperature, eCO₂ concentration, and UCE droughts influence forest C
302 dynamics individually and in combination, we implemented the following five experimental
303 scenarios, some realistic and others hypothetical, for each model (Table S1): increased



304 temperature only (+2K over ambient), eCO₂ only (600 ppm and 800 ppm), and both increased
305 temperature and eCO₂ (+2K 600 ppm; +2K 800 ppm). Temperature and eCO₂ manipulations
306 were applied as step increases over the baseline conditions, and are artificial scenarios, as
307 opposed to model-generated climate projections.

308

309 Evaluation of simulation results

310 To relate our simulation results to Fig. 1a, we compared the total biomass loss as a result
311 of each drought treatment by calculating the percentage of biomass reduction at the end of the
312 drought period relative to the baseline (no drought) simulation. To explicitly consider biomass
313 recovery rates over time, we calculated “integrated-C-loss” (Eqs. 1-3), as a result of drought
314 under current climate, which are determined based on the concepts in Fig. 1b. We defined
315 “integrated-C-loss” as the time-integrated carbon in biomass that is lost due to drought relative to
316 what the vegetation would have stored in the absence of drought. That is, it is the difference
317 between biomass in the presence of drought (B_d) at time (t) and biomass in the baseline
318 simulation (no drought; B_{base}), integrated over a defined recovery time period (in kg C m⁻²
319 yr):

$$\text{Integrated-C-loss} = \int_{t=t_1}^{t=t_2} (B_{base}(t) - B_d(t)) dt$$

320 (Eq. 1)

321 To define the bounds of integration, in Eq. 1, t_1 is defined as the time when the maximum
322 amount of plant C is lost as a result of the drought:

$$B_{base}(t_1) - B_d(t_1) = \max_t [B_{base}(t) - B_d(t)]$$

323 (Eq. 2)

324 Then, t_2 is defined implicitly as the time when 50% of the lost biomass has been recovered
325 compared to the baseline:

$$B_{base}(t_2) - B_d(t_2) = \frac{1}{2} (B_{base}(t_1) - B_d(t_1))$$

326 (Eq. 3)

327 Since all integrated-C-loss results are taken as the difference from a non-drought baseline
328 biomass (B_{base}) and all droughts will result in a loss of C.

329 We also use integrated-C-loss to examine the role of drought, temperature and eCO₂
330 change for moderating or exacerbating the impacts of drought on forest C stocks; i.e., to evaluate



331 the hypotheses illustrated in Fig. 1c. To assess these impacts of changing climates, we calculate
332 an “integrated-C-change” (Eq. 4). Defined as the difference between the integrated-C-loss due to
333 drought alone (Eqs. 1-3) under present climate, and the integrated-C-loss due to the combined
334 effects of drought and climate change (i.e., five scenarios of temperature increase and eCO₂):

$$\text{Integrated-C-change} = \text{integrated } C \text{ Loss}_{\text{Drought}} - \text{integrated } C \text{ Loss}_{\text{Drought+CC}} \quad (\text{Eq. 4})$$

335
336 Because we expect drought to reduce vegetation C stocks, and thus integrated-C-loss to
337 be negative, positive values of integrated-C-change indicate that changes in climatic drivers
338 reduced the C losses from drought (i.e., buffering effects). Negative values of integrated-C-
339 change indicate that the climate change scenario leads to either greater C losses or losses that
340 persist for longer amounts of time (i.e., magnitude and/or duration) compared to a simulation
341 with no climate change (i.e., “reference” run).

342

343 **3 Results**

344 Both models displayed nonlinear responses to drought, in concurrence with Hypothesis
345 H1, but they differ in their behavior and between sites. In general, ED2 shows sensitivity to
346 drought duration (Hypothesis H1b), while LPJ-GUESS shows a stronger sensitivity to drought
347 intensity (Hypothesis H1a). ED2’s sensitivity to the duration of drought was mild at Palo Verde
348 (Fig. 2a), and stronger at EucFACE particularly during the 4-year drought with a strong non-
349 monotonic pattern (see explanation below) (Fig. 2b). When reporting only percentage of biomass
350 loss, ED2 predicts close to no UCE response at Palo Verde; with a maximum biomass reduction
351 of only 40% during 95% precipitation removal and a 4-year drought event (i.e., UCE). LPJ-
352 GUESS shows no sensitivity to drought duration but is highly sensitive to drought intensity. C
353 loss predicted by LPJ-GUESS at Palo Verde reached a threshold at ~65% drought intensity, after
354 which forests exhibit strong biomass losses, up to 100% (Fig. 2a). At the EucFACE site, both
355 models predict a critical threshold of biomass loss at 35%-45% drought intensity, with LPJ-
356 GUESS predicting total biomass loss (up to 100%) after this drought intensity threshold (Fig.
357 2b). The EucFACE drought threshold is lower than that of the seasonally dry mixed tropical
358 forest in Palo Verde.

359 With respect to C loss over a recovering time period (integrated-C-loss), the two models
360 predict similar drought responses at Palo Verde (Fig. 2c), but not at EucFACE (Fig. 2d). At Palo



361 Verde, the similarity between models in integrated-C-loss reflected longer biomass recovery time
362 but less biomass loss in the short-term in ED2 relative to LPJ-GUESS, which predicted greater
363 biomass loss immediately after drought but shorter recovery time. With the exception of the 1-
364 year drought in ED2, both models predict similar integrated-C-loss across a range of UCEs at
365 Palo Verde, via different pathways. The integrated-C-loss metric revealed a strong non-linear
366 response to drought duration in ED2 (Fig. 2c), while this nonlinearity is less evident when only
367 examining change in biomass (Fig. 2a). The “V”-shaped patterns observed particularly in Fig.
368 2b, arise from interactions between whole-leaf phenology and stomatal responses to drought in
369 ED2. For drought intensities lower than 40%, stomatal conductance is reduced but leaves are not
370 fully shed. Leaf respiration continues, gradually depleting non-structural C pools, followed by a
371 loss of biomass. However, for higher drought intensities, leaf water potentials quickly become
372 systematically lower than leaf turgor loss points and tree cohorts shed all their leaves. This
373 strategy represents an immediate loss of C via leaf shedding, but spares the cohort from slow,
374 respiration-driven depletion of C stocks.

375

376 **3.1 Predicted model responses to UCE droughts combined with increased temperature** 377 **and/or eCO₂**

378 Relating to our second hypothesis of additional effects of warming and eCO₂, we tested
379 15 treatments in total, repeating the five climate change scenarios for each of the three drought
380 durations. With the addition of climate change impacts, ED2 remained sensitive to the duration
381 of drought, with warming negatively impacting integrated-C-change and most consistently
382 during 2- and 4-year drought durations. ED2 predicts that during the 2- and 4-year droughts at
383 EucFACE, losses are exacerbated when accompanied with warming and even with eCO₂, with
384 800 ppm having a more detrimental impact than 600 ppm (Fig. 3a-c). The average integrated-C-
385 change was -111.0 kg C m⁻² yr across all 15 treatments (Table 2). Only during the 1-year drought
386 duration did drought plus warming and eCO₂ have a buffering effect on C stocks, seen in four
387 out of our five scenarios but only during relatively modest droughts intensities (Fig. 3a; i.e.,
388 positive integrated-C-change, see also Table 2).

389 The ED2 simulations of the seasonally dry Palo Verde site (Fig. 3d-f), produced less
390 frequent negative impacts on drought and climate change driven C losses compared to
391 EucFACE, with an average integrated-C-change of -53.9 kg C m⁻² yr⁻¹ across all 15 treatments



392 (Table 2). During the 2-year drought, applying +2K with eCO₂ to 600 ppm showed a slight
393 buffering effect to droughts and the most consistent positive integrated-C-change (Fig. 3e; Table
394 2). Interestingly, an increase in only eCO₂ to 800 ppm (no warming) when applied with the 2-
395 and 4-year droughts resulted in the largest loss in integrated-C-change (Fig. 3e-f), larger than the
396 expected ‘most severe’ scenario; +2K and 800 ppm.

397 Similar to ED2, the LPJ-GUESS model showed a nearly complete negative response in
398 integrated-C-change as a result of UCE drought and scenarios of warming and eCO₂ at the
399 EucFACE site (Fig. 3g-i), but mixed and more muted results at Palo Verde (Fig. 3j-l, Table 2).
400 The average integrated-C-change relative to the reference case was -95.4 at EucFACE and -7.8
401 kg C m⁻² yr at Palo Verde, both less negative compared to ED2. One notable pattern was up until
402 a drought intensity threshold of ~40%, the climate scenarios had no effect or response in
403 integrated-C-change at EucFACE, and the muted response from warming and eCO₂ Palo Verde,
404 compared to ED2. Surprisingly, the +2K scenario switched the integrated-C-change to positive,
405 compared to the reference case (Fig. 3g-i; red lines), potentially a physiological process in the
406 model to increased temperatures only that signals an anomalous resiliency response. Similar to
407 the results with no climate change, LPJ-GUESS remained sensitive to the intensity of drought,
408 with ~40% precipitation reduction being a threshold.

409 The models and sites differed with regard to SO and MO responses to increasing drought
410 severity and its interactions with warming and eCO₂ (related to conceptual Fig. 1d). ED2 showed
411 a more consistent MO response during UCEs and with additional warming and eCO₂ (Fig. 3;
412 negative integrated-C-change), especially at EucFACE, suggesting these ecosystems will remain
413 in a depressed carbon condition driving vegetation mortality, and/or longer recoveries. LPJ-
414 GUESS produced more opportunities for SO with climate change. For example, at EucFACE
415 CO₂ fertilization created small SO periods that then led to MO with increasing drought severities,
416 and at Palo Verde all +2K and 600 ppm led to a SO (Fig. 3j-l; Table 2).

417 Both models predicted that C losses due to drought interactions with increased
418 temperature and eCO₂ were less severe at the seasonally dry Palo Verde site compared to the
419 somewhat less seasonal, more humid EucFACE site (Table 2), which could be attributed to
420 higher diversity in PFT physiology at Palo Verde. Palo Verde’s community composition that
421 emerged following drought included either three (LPJ-GUESS) or four (ED2) PFTs, while only a
422 single PFT existed at EucFACE. With rising temperatures under climate change, UCEs will be



423 hotter and drier. Nine out of the twelve simulations with both +2K and 600 ppm CO₂, and all but
424 one +2K and 800 ppm CO₂ produced a negative integrated-C-change, implying stronger C losses
425 and/or longer recovery times when droughts are exacerbated by increasing temperatures (Table
426 2).

427

428 **4 Discussion**

429 We applied two vegetation demographic models (VDMs) to explore two hypotheses
430 regarding a range of modeled response of terrestrial ecosystems to unprecedented climate
431 extremes (UCEs). Key model results include strong nonlinearities (Hypothesis H1) in C response
432 to extreme drought *intensities* in LPJ-GUESS and alternatively drought *durations* in ED2 (at one
433 of two sites), with differences in thresholds between the two models and ecosystems. These
434 nonlinearities may arise from multiple mechanisms that we begin to investigate here, including
435 shifts in plant hydraulics or other functional traits, C allocation, phenology, and stand
436 demography, all which vary among ecosystem types. The models also show exacerbated biomass
437 loss and recovery times in the majority of our scenarios of warming and eCO₂, supporting
438 Hypothesis H2. Below, we elucidate the underlying mechanisms that drive simulated ecosystem
439 response to UCEs based on our simulation results and observational evidence from the literature.
440 We focus on two temporal stages of the UCE: The pre-drought ecosystem stage characterized as
441 the quasi-stable state of the ecosystem prior to a UCE, which can mediate ecosystem resistance
442 and disturbance impact, and the post-drought recovery stage (Table 1).

443

444 **4.1 The role of ecosystem processes and states prior to UCEs**

445 **4.1.1 The role of phenology and phenological strategies prior to UCEs:**

446 Observations show that different levels of deciduousness contribute to alternative
447 strategies for tropical tree response to water stress (Williams et al., 2008). For example, during
448 the severe 1997 El Nino drought, brevi-deciduous trees and deciduous stem-succulents within a
449 tropical dry site in Guanacaste Costa Rica retained leaves during the extreme wet-season
450 drought, behaving differently than during normal dry seasons (Borchert et al., 2002). Both
451 models here predict that neither seasonal deciduousness, nor drought-deciduous phenology at the
452 seasonally dry tropical forest, Palo Verde (which consists of trees with different leaf



453 phenological strategies), act to buffer the forest from a large drop in LAI during UCEs (Fig. S1a-
454 b). Even with this large decrease in LAI, ED2 predicted a very weak biomass loss at the time of
455 UCEs (Fig. 2a), suggesting large-scale leaf loss is not a direct mechanism of plant mortality in
456 ED2. At the EucFACE site prior to the simulated extreme drought, LAI was stable in ED2, while
457 LPJ-GUESS displayed strong inter-annual variability in LAI (Fig. S1a-b). This capability of
458 large swings in LAI, and the larger LAI drop (3.0 to 1.7) by LPJ-GUESS could potentially
459 contribute to the considerable mortality response at EucFACE. Models might better capture the
460 different plant phenological responses to UCEs if the PFT phenology schemes better represented
461 morphological and physiological characteristics relevant to plant-water relations (e.g., leaf age;
462 retention of young leaves even during extreme droughts; Borchert et al., (2002); variation in
463 hydraulic traits as a function of leaf habit Vargas et al., (2021)) (Table 3).

464

465 **4.1.2 The role of plant hydraulics prior to UCEs:**

466 Susceptibility of plants to hydraulic stress is one of the strongest determinants of
467 vulnerability to drought, with loss of hydraulic conductivity being a major predictor of drought
468 mortality in temperate (McDowell et al., 2013; Anderegg et al., 2015; Sperry and Love, 2015;
469 Venturas et al., 2021) and tropical forests (Rowland et al., 2015; Adams et al., 2017b), as well as
470 a tractable mortality mechanism to represent in process-based models (Choat et al., 2018,
471 Kennedy et al., 2019). Both LPJ-GUESS and ED2 exhibited a wide range in amount and pattern
472 of plant-available-water prior to drought (Fig. S1c-d), leading to large differences in UCE
473 response. LPJ-GUESS predicted lower total plant-available-water at both sites compared to ED2,
474 and subsequently simulated a greater increase in plant-available-water right after the UCEs as a
475 result of greater mortality and decrease in water demand. Due to ED2 using a static mortality
476 threshold from conductivity loss (88%), it likely does not accurately reproduce the wide range of
477 observations of drought-induced mortality. In ED2, large trees, with longer distances to transport
478 water, were at higher risk and suffered higher mortality (Fig. S3), demonstrating how stand
479 demography and size structure can play an important role in ecosystem models (Fisher et al.,
480 2018). There are strong interdependencies and related mechanisms connecting both hydraulic
481 failure (e.g., low soil moisture availability) and C limitation (e.g., stomatal closure) during
482 drought (McDowell et al., 2008; Adams et al., 2017b), and these interactions should be
483 incorporated in ecosystem modeling and further explored (Table 3).



484 **4.1.3. The role of carbon allocation prior to UCEs:**

485 Plants have a variety of strategies to buffer vulnerability to water and nutrient stress
486 caused by extreme droughts, such as allocating more C to deep roots (Joslin et al., 2000; Schenk
487 and Jackson, 2005), investing in mycorrhizal fungi (Rapparini and Peñuelas, 2014), or reducing
488 leaf area without shifting leaf nutrient content (Pilon et al., 1996). Alternatively, presence of
489 deep roots doesn't necessarily lead to deep soil moisture utilization, as seen in a 6-year
490 Amazonian throughfall exclusion experiment where deep root water uptake was still limited,
491 even with high volumetric water content (Markewitz et al., 2010). Elevated CO₂ alone will
492 enhance growth and water-use efficiency (Keenan et al., 2013), reducing susceptibility to
493 drought. However, such increased productivity within a forest stand, and associated structural
494 overshoot during favorable climate windows, can also be reversed by increased competition for
495 light, nutrients, and water during unfavorable UCEs – potentially leading to mortality overshoot
496 (Fig. 1d) and higher C loss. Mortality overshoot could be an explanation for the negative
497 integrated-C-change (i.e., C loss) in the majority of eCO₂-only simulations (18 out of 24
498 scenarios; Table 2).

499 Effects of CO₂ fertilization on plant C allocation strategies are uncertain. As a result,
500 ecosystem models differ in their assumptions on controls of C allocation in response to eCO₂,
501 leading to divergent plant C use efficiencies (Fleischer et al., 2019). Global scale terrestrial
502 models are beginning to include dynamic C allocation schemes, over fixed ratios, that account
503 for concurrent environmental constraints on plants, such as water, and adjust allocation based on
504 resource availability (Weng et al., 2015; Zhu et al., 2019), but the representation of C allocation
505 is still debated and progressing (De Kauwe et al., 2014; Montané et al., 2017; Reyes et al., 2017).
506 It is worth investigating the differences between C allocation based on the allometric partitioning
507 theory (i.e., allocation follows a power allometry function between plant size and organs which
508 is insensitive to environmental conditions; Niklas, 1993), as an alternative to ratio-based optimal
509 partitioning theory (i.e., allocation to plant organs based on the most limiting resources)
510 (McCarthy and Enquist, 2007) or fixed ratios (Table 3), particularly due to VDMs substantial use
511 of allometric relationships. A meta-analysis of 164 studies found that allometric partitioning
512 theory outperformed optimal partitioning theory in explaining drought-induced changes in C
513 allocation (Eziz et al., 2017).

514



515 4.1.4 The role of plant carbon storage prior to UCEs:

516 Studies of neotropical and temperate seedlings show that pre-drought storage of non-
517 structural carbohydrates (NSCs) provides the resources needed for growth, respiration
518 osmoregulation, and phloem transport when stomata close during subsequent periods of water
519 stress (Myers and Kitajima, 2007; Dietze and Matthes, 2014; O'Brien et al., 2014). Furthermore,
520 direct correlations have been shown between NSC depletion and embolism accumulation, and
521 the degree of pre-stress reserves and utilization of soluble sugars (Tomasella et al., 2020). The
522 amount of NSC storage required to mitigate plant mortality during C starvation and interactions
523 with hydraulic failure from severe drought is difficult to quantify, due to the many roles of NSCs
524 in plant function and metabolism (Dietze and Matthes, 2014). For example, NSCs were not
525 depleted after 13 years of experimental drought in the Brazilian Amazon (Rowland et al., 2015).
526 As atmospheric CO₂ increases with climate change, NSC concentrations may increase, as seen in
527 manipulation experiments (Coley, 2002), but interactions with heat, water stress, enhanced leaf
528 shedding, and nutrient limitation complicates this relationship, and needs to be further explored.
529 Despite the recognition of the critical role that plant hydraulic functioning and NSCs play in tree
530 resilience to extremes, knowledge gaps and uncertainties preclude fully incorporating these
531 processes into ecosystem models.

532 Compared to ED2, LPJ-GUESS predicted low plant carbon storage (a model proxy for
533 NSCs) prior to and during drought, and at times became negative, thereby creating C costs (Fig.
534 S2a-b), leading to C starvation and potentially explaining the larger biomass loss in LPJ-GUESS
535 at both sites. Alternatively, ED2 maintained higher levels of NSCs providing a buffer to stress,
536 and mitigating the negative effects of drought. Maintenance of NSCs in ED2, even during
537 prolonged drought (at EucFACE) is due to: (1) trees resorbing a fraction of leaf C during leaf
538 shedding, (2) no maintenance costs for NSC storage in the current version, and (3) no allocation
539 of NSCs to structural growth until NSC storage surpasses a threshold (the amount of C needed to
540 build a full canopy of leaves and associated fine roots), allowing for a buffer to accumulate. In
541 LPJ-GUESS, accumulation and depletion of NSC is recorded as a 'C debt' being paid back in
542 later years. The contrasting responses of the two models to drought, and the likely role of NSCs
543 in explaining differences in model behavior, highlights the need to better understand NSC
544 dynamics and to accurately represent the relevant processes in models (Richardson et al., 2013;
545 Dietze and Matthes, 2014). More observations of C accumulation patterns and how/where NSCs



546 drive growth, respiration, transport and cellular water relations would enable a more realistic
547 implementation of NSC dynamics in models (Table 3).

548

549 **4.1.5 Role of functional trait diversity prior to UCEs:**

550 Currently LPJ-GUESS simulates the Palo Verde community using three PFTs, while ED2 uses
551 four PFTs that differ in photosynthetic and hydraulic traits. The community composition simulated by
552 ED2 is shown to be more resistant to UCEs compared to LPJ-GUESS (Fig. 4), perhaps due to
553 relatively higher functional diversity. This additional diversity helps to buffer ecosystem response to
554 drought by allowing more tolerant PFTs to benefit from reductions in less-tolerant PFTs, thus
555 buffering reductions in ecosystem function (Anderegg et al., 2018). Higher diversity ecosystems were
556 found to protect individual species from negative effects of drought (Aguirre et al., 2021) and enhance
557 productivity resilience following wildfire (Spasojevic et al., 2016); thus, functionally diverse
558 communities may be key to enhancing tolerance to rising environmental stress.

559 Recent efforts to consolidate information on plant traits (Reich et al., 2007; Kattge et al., 2011)
560 have contributed to identifying relationships that can impact community-level drought responses
561 (Skelton et al., 2015; Anderegg et al., 2016a; Uriarte et al., 2016; Greenwood et al., 2017), such as
562 life-history characteristics, and strategies of resource acquisition and conservation as predictors of
563 ecosystem resistance (MacGillivray et al., 1995; Ruppert et al., 2015). While adding plant trait
564 complexity in ESMs may be required to accurately simulate key vegetation dynamics, it necessitates
565 more detailed parameterizations of processes that are not explicitly resolved (Luo et al., 2012). Further
566 investigation of how VDMs represent interactions leading to functional diversity shifts is crucial to
567 this issue. Enquist and Enquist, (2011), as an example, show that long-term patterns of drought (20-
568 years) have led to increases in drought-tolerant dry forest species, which could modulate resistance to
569 future droughts. Higher diversity of plant physiological traits and drought-resistance strategies is
570 expected to enhance community resistance to drought, and models should account for shifts in diverse
571 functionality (Table 3).

572

573 **4.2 The role of ecosystem processes and states in post-UCE recovery**

574 **4.2.1 The role of soil water resources post-UCEs:**



575 Our simulation results generally demonstrated a fast recovery of plant-available-water
576 and LAI at both sites (Fig. S1). Annual plant-available-water substantially increased right after
577 drought by an average of 163 mm at Palo Verde and 213 mm at EucFACE in the LPJ-GUESS
578 simulations, compared to much lower increases in ED2 (50 mm and 12 mm at Palo Verde and
579 EucFACE). This increase in available water post-drought can be attributed to reduced stand
580 density and water competition (Fig. S2c-d; diamonds vs. circles), alleviating the demand for soil
581 resources (water) and subsequent stress, which has also been shown in observations (McDowell
582 et al., 2006; D'Amato et al., 2013). After large canopy tree mortality events there can be
583 relatively rapid recovery of forest biogeochemical and hydrological fluxes (Biederman et al.,
584 2015; Anderegg et al., 2016b; Biederman et al., 2016). These crucial fluxes strongly influence
585 plant regeneration and regrowth, which can buffer ecosystem vulnerability to future extreme
586 droughts. However, this enhanced productivity has a limit. In a scenario where UCEs continue to
587 intensify, causing greater reductions in soil water and reduced ecosystem recovery potential, the
588 SO growth that typically occurs after UCEs may be dampened (Fig. 1d). In water-limited
589 locations, similar to the dry forest sites used here, initial forest recovery from droughts were
590 faster due to thinning induced competitive-release of the surviving trees, and shallow roots not
591 having to compete with neighboring trees for water, allowing for more effective water user
592 (Tague and Moritz, 2019), stressing the importance of root competition and distribution in
593 models (Goulden and Bales, 2019). Tague and Moritz, (2019) also reported that this increased
594 water use efficiency and SO ultimately lead to water stress and related declines in productivity,
595 similar to the MO concept (Jump et al., 2017; McDowell et al., 2006). Since a core strength of
596 VDMs is predicting stand demography during recovery, improved quantification of density-
597 dependent competition following stand dieback would be beneficial for model benchmarking
598 (Table 3).

599

600 **4.2.2 The role of lagged turnover and secondary stressors post-UCes:**

601 Time lags in forest compositional response and survival to drought could indicate
602 community resistance or shifts to more competitive species and competitive exclusion. During a
603 15-year recovery period from extreme drought at Palo Verde, LPJ-GUESS predicted an increase
604 in stem density (stems $\text{m}^2 \text{yr}^{-1}$) (Fig. S2c) compared to ED2, which predicted almost no impact in



605 stem recovery. The mortality “spike” in ED2 due to drought was muted and slightly delayed,
606 contributing to ED2’s lower biomass loss and more stable behavior of plant processes over time
607 at Palo Verde. At EucFACE, both models exhibited a pronounced lag effect in stem turnover
608 response, i.e. ~8-12 years after drought (Fig. S2d). After about a decade, strong recoveries and
609 increased stem density occurred, which in ED2 was followed by delayed mortality/thinning of
610 stems. Delayed tree mortality after droughts are common due to optimizing carbon allocation and
611 growth (Trugman et al., 2018), but typically only up to several years post-drought, not a decade
612 or more as seen in the model.

613 The versions of the VDMs used here do not directly consider post-drought secondary
614 stressors such as infestation by insects or pathogens, and the subsequent repair costs due to stress
615 damage, which could substantially slow the recovery of surviving trees. Forest ecologists have
616 long recognized the susceptibility of trees under stress, particularly drought, to insect attacks and
617 pathogens (Anderegg et al., 2015). Tight connections between drought conditions and increased
618 mountain pine beetle activity have been observed (Chapman et al., 2012; Creeden et al., 2014),
619 and can ultimately lead to increased tree mortality (Hubbard et al., 2013). Leaf defoliation is a
620 major concern from insect outbreaks following droughts, and can have large impacts on C
621 cycling, plant productivity, and C sequestration (Amiro et al., 2010; Clark et al., 2010; Medvigy
622 et al., 2012). Implementing these secondary stressors in models could slow the rate of post-UCE
623 recovery and lead to increased post-UCEs tree mortality.

624

625 **4.2.3 The role of stand demography post-UCEs:**

626 Change in stand structure is an important model process to capture, because large trees
627 have important effects on C storage, community resource competition, and hydrology
628 (Wullschleger et al., 2001) (Table 3), and maintaining a positive carbohydrate balance is
629 beneficial in sustaining (or repairing) hydraulic viability (McDowell et al., 2011). There is
630 increasing evidence, both theoretical (McDowell and Allen, 2015) and empirical (Bennett et al.,
631 2015; Rowland et al., 2015; Stovall et al., 2019), that large trees (particularly tall trees with high
632 leaf area) contribute to the dominant fraction of dead biomass after drought events. Under rising
633 temperatures (and decreasing precipitation), VPD will increase, leading to a higher likelihood of
634 large tree death (Eamus et al., 2013; Stovall et al., 2019), driving MO events as hypothesized in



635 Fig. 1d. Consistent with this expectation, ED2 predicted that the largest trees (>100 cm)
636 experienced the largest decreases in basal area to compared to all other size classes (Fig. S3).
637 This drought-induced partial dieback and whole-tree mortality of dominant trees has substantial
638 impacts on stand-level C dynamics, as long-term sequestered C is liberated during the decay of
639 new dead wood (Palace et al., 2008; Potter et al., 2011). In ED2, the intermediate size class (60 -
640 80 cm) increased in basal area following large-tree death, taking advantage of the newly open
641 canopy space. However, small size classes do not necessarily benefit from canopy dieback. For
642 example, in a dry tropical forest, prolonged drought led to a decrease in understory species and
643 small-sized stems (Enquist and Enquist, 2011).

644

645 **4.2.4 The role of functional trait diversity & plant hydraulics post-UCEs:**

646 During the recovery phase from disturbance, competition will likely shift the plant
647 community towards one that is composed of opportunistic, fast-growing pioneer tree species,
648 grasses (Shiels et al., 2010; Carreño-Rocabado et al., 2012), and/or deciduous species, as also
649 seen in previous model results (Hickler et al., 2004). In the treatments presented here, deciduous
650 PFT types were also the strongest to recover after 15 years in both models, surpassing pre-
651 drought values (Fig. 4). It should be noted that ED2 exhibited a strong recovery in the evergreen
652 PFT as well (over two other deciduous PFT types), inconsistent with the above literature (Fig.
653 4b). PFTs in ED2 respond to drought conditions via stomatal closure and leaf shedding,
654 buffering stem water potentials from falling below a set mortality threshold (i.e., 88% of loss in
655 conductivity). This conductivity threshold may need to be reconsidered if further examination
656 reveals an unrealistic advantage under drought conditions for evergreen trees, which exhibited a
657 lower impact from droughts (compared to deciduous and brevi-deciduous PFTs) in ED2.

658 Recovery of surviving trees could be hindered by the high cost of replacing damaged
659 xylem associated with cavitation (McDowell et al., 2008; Brodribb et al., 2010). Many studies
660 have identified “drought legacy” effects of delayed growth or gross primary productivity
661 following drought (Anderegg et al., 2015; Schwalm et al., 2017) and the magnitude of these
662 legacies across species correlates with the hydraulic risks taken during drought itself (Anderegg
663 et al., 2015). The conditions under which xylem can be refilled remain controversial, but it seems
664 likely that many species, particularly gymnosperms, may need to entirely replace damaged



665 xylem (Sperry et al., 2002), and trees worldwide operate within narrow hydraulic safety margins,
666 suggesting that trees in all biomes are vulnerable to drought (Choat et al., 2012). The amount of
667 damaged xylem from a given drought event and recovery rates also vary across trees of different
668 sizes (Anderegg et al., 2018).

669 Plasticity in nutrient acquisition traits, intraspecific variation in plant hydraulic traits
670 (Anderegg et al., 2015), and changes in allometry (e.g., Huber values) can have large effects on
671 acclimation to extreme droughts. This suggests some capacity for physiological adaptation to
672 extreme drought, as seen by short-term negative effects from drought and heat extremes being
673 compensated for in the longer term (Dreesen et al., 2014). Still, given the shift towards more
674 extreme droughts with climate change, vegetation mortality thresholds are likely to be exceeded,
675 as reported in Amazonian long-term plots where mortality of wet-affiliated genera has increased
676 while simultaneously new recruits of dry-affiliated genera are also increasing (Esquivel-Muelbert
677 et al., 2019). Increasing occurrences of heat events, water stress and high VPD will lead to
678 extended closure of stomata to avoid cavitation, progressively reducing CO₂ enrichment benefits
679 (Allen et al., 2015). Where CO₂ fertilization has been seen to partially offset the risk of
680 increasing temperatures, the risk response was mediated by plant hydraulic traits (Liu et al.,
681 2017), yet interactions with novel extreme droughts were not considered. The VDM simulations
682 suggest that the combination of elevated warming and eCO₂ will exacerbate consequences of
683 UCEs by reductions in both C stocks and post-drought biomass recovery speeds (Fig. 3).
684 Therefore, future UCE recovery may not be easily predicted from observations of historical post-
685 disturbance recovery. An associated area for further investigation is to better understand the
686 hypothesized interplay between amplified mortality from hotter UCEs followed by structural
687 overshoot regrowth during wetter periods (Fig. 1d), which could potentially buffer net ecosystem
688 C impacts through time (Table 3).

689

690 **5 Conclusions**

691 Model limitations and unknowns exposed by our simulations highlight current challenges
692 in our ability to understand and forecast UCE effects on ecosystems. These limitations reflect a
693 general lack of empirical experiments focused on UCEs. Insufficient data means that relevant
694 processes may currently be poorly represented in models, and models may then misrepresent C
695 losses during UCEs. The two VDMs used here had different sensitivities to drought duration and



696 intensity. These model uncertainties could potentially be addressed by improved datasets on
697 thresholds of conductivity loss at high drought intensities, the role of trait diversity (e.g. different
698 strategies of drought deciduousness) in buffering ecosystem drought responses, and a better
699 grasp of plant storage stocks before, during, and after multi-year droughts. Our study takes some
700 initial steps to identify and assess model uncertainties in terms of mechanisms and magnitudes of
701 responses to UCEs, which can then be used to inform and develop field experiments targeting
702 key knowledge gaps as well as to prioritize ongoing model development (Table 3). This iterative
703 model-experiment framework offers strong potential to drive progress in improving our
704 understanding of terrestrial ecosystem responses to UCEs and climate feedbacks, while
705 informing the development of the next generation of models.



706 *Code Availability.* The source code for the ED2 model can be downloaded and available publicly
707 at <https://github.com/EDmodel/ED2>. The source code for the LPJ-GUESS model can be
708 downloaded and available publicly at <http://web.nateko.lu.se/lpj-guess/download.html>. All model
709 simulation data will be available in a Dryad repository.
710

711 *Data Availability.* Authors received the required permissions to use the site level meteorological
712 data used in this study. Otherwise, no ecological or biological data were used in this study.
713

714 *Author Contributions.* JH wrote the manuscript with significant contributions from AR, BS, JD,
715 DM, with input and contributions from all authors. XX and MM were the primary leads running
716 the model simulations, with model assistance and strong feedback from DM and BS. All authors
717 made contributions to this article, and agree to submission.
718

719 *Competing Interests.* The contact author has declared that neither they nor their co-authors have
720 any competing interests.
721

722 *Special Issue Statement.* Special Issue titled “Ecosystem experiments as a window to future
723 carbon, water, and nutrient cycling in terrestrial ecosystems”
724

725 *Financial Support:* Funding for the meetings that facilitated this work was provided by NSF-
726 DEB-0955771: An Integrated Network for Terrestrial Ecosystem Research on Feedbacks to the
727 Atmosphere and ClimatE (INTERFACE): Linking experimentalists, ecosystem modelers, and
728 Earth System modelers, hosted by Purdue University; as well as Climate Change Manipulation
729 Experiments in Terrestrial Ecosystems: Networking and Outreach (COST action ClimMani –
730 ES1308), led by the University of Copenhagen. J.A. Holm’s time was supported as part of the
731 Next Generation Ecosystem Experiments-Tropics, funded by the U.S. Department of Energy,
732 Office of Science, Office of Biological and Environmental Research under Contract DE-AC02-
733 05CH11231. AR acknowledges funding from CLIMAX Project funded by Belmont Forum and
734 the German Federal Ministry of Education and Research (BMBF). BS and MM acknowledge
735 support from the Strategic Research Area MERGE. W.R.L.A. acknowledges funding from the
736 University of Utah Global Change and Sustainability Center, NSF Grant 1714972, and the
737 USDA National Institute of Food and Agriculture, Agricultural and Food Research Initiative
738 Competitive Programme, Ecosystem Services and Agro-ecosystem Management, grant no. 2018-
739 67019-27850. JL acknowledges support from the Northern Research Station of the USDA Forest
740 Service (agreement 16-JV-11242306-050) and a sabbatical fellowship from sDiv, the Synthesis
741 Centre of iDiv (DFG FZT 118, 202548816). CDA acknowledges support from the USGS Land
742 Change Science R&D Program.
743

744 *Acknowledgements.* We thank Belinda Medlyn and David Ellsworth of the Hawkesbury Institute
745 for the Environment, Western Sydney University, for providing the meteorological forcing data
746 series for the EucFACE site, a facility supported by the Australian Government through the
747 Education Investment Fund and the Department of Industry and Science, in partnership with
748 Western Sydney University.
749



750 **Table 1.** Hypothesized plant processes and ecosystem state variables affecting pre-drought
 751 resistance and post-drought recovery in the context of unprecedented climate extremes (UCEs).
 752 The “Included in Model?” column indicates which processes or state variables are represented in
 753 each of the two models studied in this paper. Mechanisms listed in the two right columns refer to
 754 real ecosystems and are not necessarily represented in models, even if the process or state
 755 variable is represented in a given model. Contents of the table are based on a non-exhaustive
 756 literature review, expert knowledge, and modeling results presented here. Symbols refer to the
 757 following literature sources: * Borchert et al., 2002; Williams et al., (2008); ** Dietze and
 758 Matthes, (2014); O’Brien et al., 2014; *** ENQUIST and ENQUIST, (2011); Greenwood et al.,
 759 (2017); Powell et al., (2018); ^ Rowland et al., (2015); McDowell et al., (2013); Anderegg et al.,
 760 (2015); ^^ Joslin et al., 2000; Markewitz et al., (2010); ^^^ Powell et al., (2018); ^^^^ Bennett et
 761 al., (2015); Rowland et al., (2015); ~ Hubbard et al., (2013); ~ ~ McDowell et al., 2006,
 762 D’Amato et al., (2013); + Vargas et al., (2021).

Process or State Variable	Included in model?	Mechanisms affecting pre-UCE drought resistance influencing impact	Mechanisms affecting post-UCE drought recovery
Processes			
1) Phenology Schemes	ED2: Yes LPJ-G: Yes	Leaf area and metabolic activity modulate vulnerability to death; drought-deciduousness reduces vulnerability to drought *, with higher water potential at turgor loss point and leaf vulnerability to embolism +	Leaf lifespan tends to increase from pioneer to late-successional species in some ecosystems (e.g., tropical forests)
2) Plant Hydraulics	ED2: Yes LPJ-G: No	Cavitation resistance traits ^; turgor loss, hydraulic failure (stem embolism) lead to increased plant mortality and enhanced vulnerability to secondary stressors	Replacement cost of damaged xylem slows recovery of surviving trees
3) Dynamic Carbon Allocation	ED2: Yes LPJ-G: Yes	Increased root allocation could offset soil water deficit under gradual onset of drought ^^	Allocation among fine roots, xylem, & leaves affects recovery time & GPP/LAI trajectory



4) Non-Structural Carbohydrate (NSC) Storage	ED2: Yes LPJ-G: Yes	Buffers C starvation mortality due to reduced primary productivity; maintenance of hydraulic function & avoiding hydraulic failure **	Low NSC could increase vulnerability to secondary stressors during recovery
State Variables			
1) Plant-Soil Water Availability	ED2: Yes LPJ-G: Partly	Low soil water potential increases risk of tree C starvation, turgor loss and hydraulic failure	After stand dieback reduced demand for soil resources &/or reduced shading. Increased soil water enhances regeneration/regrowth, buffers vulnerability to long-term drought ~ ~
2) Plant Functional Diversity	ED2: Yes LPJ-G: Yes	Presence of drought-tolerant species modulates resistance at community level. Shallow-rooting species more vulnerable ^^ ***	Changed resource spectra shift competitive balance in favor of grasses and pioneer trees
3) Stand Demography	ED2: Yes LPJ-G: Yes	Larger tree size enhances vulnerability to drought and secondary stressors due to higher maintenance costs ^^ ^^	Mortality of canopy individuals favors understory species and smaller size-classes
4) Compounding Stressors	ED2: No LPJ-G: No	Reduced resistance to insects and pathogens due to physiological/mechanical/ hydraulic damage & depletion of NSC	Infestation by insects and pathogens, repair of damage due to secondary stressors, slows recovery of surviving trees ~



764 **Table 2** Impact of eCO₂ and/or temperature on the integrated-C-change (kg C m⁻² yr) relative to
 765 drought treatments with no additional warming or eCO₂, for both models, and both sites seen in
 766 Fig. 3. Quantified as average and minimum integrated-C-change across all 20 drought intensities
 767 for step-change scenarios of warming and eCO₂. The percentage of each scenario that was
 768 negative in integrated-C-change (i.e., decreases in C loss). Green values represent positive
 769 integrated-C-change.

<i>EucFACE</i>	<i>ED2</i>			<i>LPJ-GUESS</i>			
	Average integrated C change	Largest integrated C change	% climate scenario was negative	Average integrated C change	Largest integrated C change	% climate scenario was negative	
1 year	600 ppm	2.2	0.0	33.3	-74.6	-396.6	36.8
	800 ppm	-10.6	-73.0	50.0	-124.1	-416.0	57.9
	2K	2.3	-0.5	16.7	21.3	-20.8	15.8
	2K, 600 ppm	0.5	-8.2	61.1	-67.5	-201.5	78.9
	2K, 800 ppm	1.8	-0.4	22.2	-145.9	-400.1	47.4
2 year	600 ppm	-105.6	-456.7	77.8	-85.2	-260.6	63.2
	800 ppm	-199.0	-522.9	83.3	-106.3	-350.1	42.1
	2K	-10.3	-34.7	77.8	14.2	-35.2	31.6
	2K, 600 ppm	-204.9	-666.1	77.8	-47.6	-128.8	84.2
	2K, 800 ppm	-12.4	-61.6	50.0	-167.0	-421.9	68.4
4 year	600 ppm	-125.5	-306.2	83.3	-122.6	-277.4	94.7
	800 ppm	-277.1	-423.3	100.0	-212.2	-523.7	89.5
	2K	-61.8	-188.6	72.2	12.9	-13.8	31.6
	2K, 600 ppm	-385.9	-674.2	94.4	-79.1	-197.3	94.7
	2K, 800 ppm	-277.9	-737.7	72.2	-247.0	-503.8	100.0
Average	-111.0	-277.0	64.8	-95.4	-276.5	62.5	
<i>Palo Verde</i>	<i>ED2</i>			<i>LPJ-GUESS</i>			
1 year	600 ppm	-1.6	-6.2	77.8	-11.0	-32.4	78.9
	800 ppm	6.7	-0.2	11.1	-39.2	-154.0	100.0
	2K	-1.0	-15.3	38.9	-33.4	-75.1	100.0
	2K, 600 ppm	2.5	-1.1	22.2	6.5	-4.6	52.6
	2K, 800 ppm	-6.6	-16.6	77.8	-121.1	-237.7	100.0
2 year	600 ppm	15.1	-16.7	38.9	27.3	-6.0	10.5
	800 ppm	-229.2	-756.6	66.7	20.6	-17.2	26.3
	2K	-8.2	-71.8	50.0	32.0	-12.7	15.8
	2K, 600 ppm	24.8	-5.7	11.1	36.2	-1.2	5.3
	2K, 800 ppm	-152.9	-348.1	77.8	8.0	-54.5	36.8
4 year	600 ppm	-11.1	-37.3	94.4	3.4	-25.1	26.3
	800 ppm	-260.2	-694.8	94.4	-25.2	-132.6	57.9
	2K	-39.0	-133.8	66.7	-7.7	-45.9	68.4
	2K, 600 ppm	1.0	-16.4	38.9	6.1	-4.1	31.6
	2K, 800 ppm	-148.5	-429.3	83.3	-20.0	-75.5	78.9
Average	-53.9	-170.0	56.7	-7.8	-58.6	52.6	

770



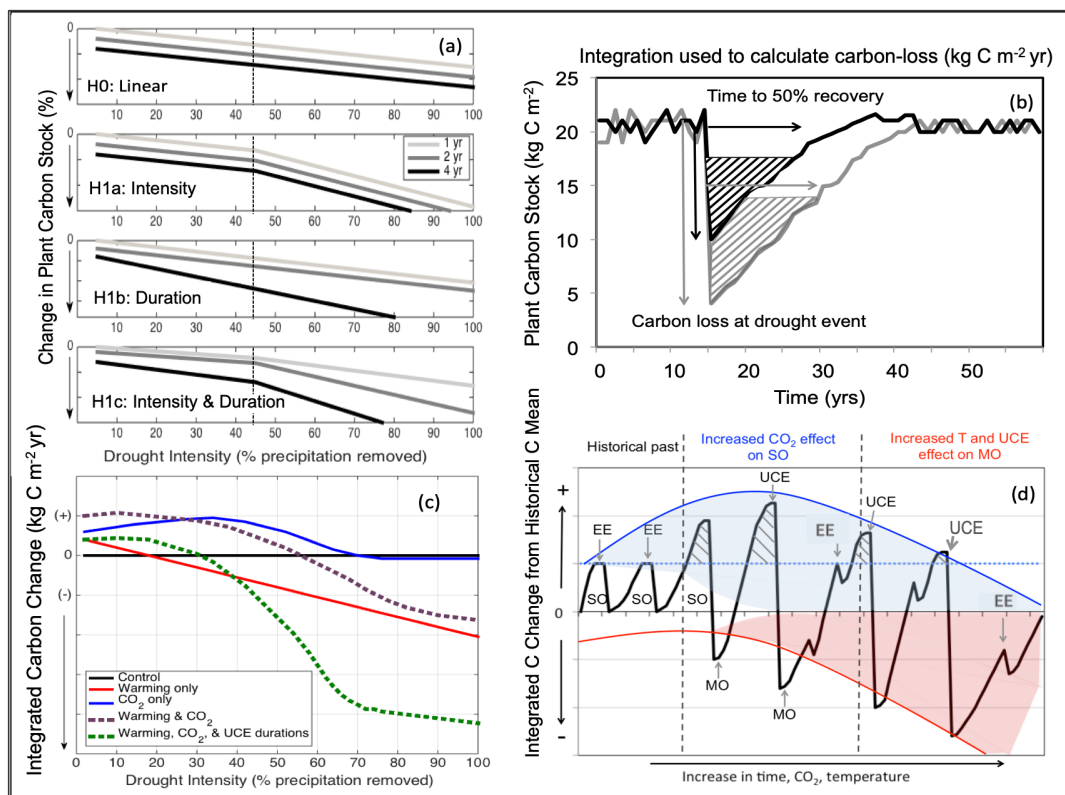
771 **Table 3** Summary of suggestions emerging from the hypothetical drought simulations used here
 772 of the driving mechanisms (e.g., ecosystem or plant processes and state variables) to explore for
 773 future research in manipulation experiments, data collection, and model development and testing,
 774 as related to furthering our understanding of UCE resistance and recovery.

UCE Drought Resistance & Recovery Summary	
Processes	Suggestions of driving mechanisms to further explore in data and models
1) Phenology Schemes	Represent morphological and physiological traits relevant to plant-water relations; drought- deciduousness can reduce vulnerability to drought; phenology of evergreens needs more investigation.
2) Plant Hydraulics	Interactions between hydraulic failure (e.g. low soil moisture availability) and C limitation (e.g. stomatal closure) during drought should be included in models. Account for turgor loss, hydraulic failure traits, costs to recover damaged xylem.
3) Dynamic Carbon Allocation	C allocation based on the allometric partitioning theory in addition, or replacing ratio-based optimal partitioning theory, and fixed ratios. Explore root allocation that could offset soil water deficits.
4) Non-structural Carbohydrate (NSC) Storage	Deciding best practices for NSC representation in models. Better understanding of NSC storage required to mitigate plant mortality during C starvation and interactions with avoiding hydraulic failure during severe droughts.
States Variables	
1) Plant-Soil Water Availability	Better quantification of the amount and accessibility of plant-available water for surviving trees, and tradeoff between increased structural productivity but vulnerability to subsequent droughts. Future relevance, or benefit, of lower water demand due to thinning with UCEs.
2) Plant Functional Diversity	Understand how higher diversity of plant physiological traits and drought-resistance strategies will enhance community resistance to drought; models still need to account for shifts in diverse functionality, including deciduousness shifts and interplay of regrowth structural overshoot followed by amplified mortality from hotter UCEs.
3) Stand Demography	Large trees more vulnerable to drought; need data on changes in C stock with UCEs in high-density smaller tree stands vs. stands with larger trees.

775



776

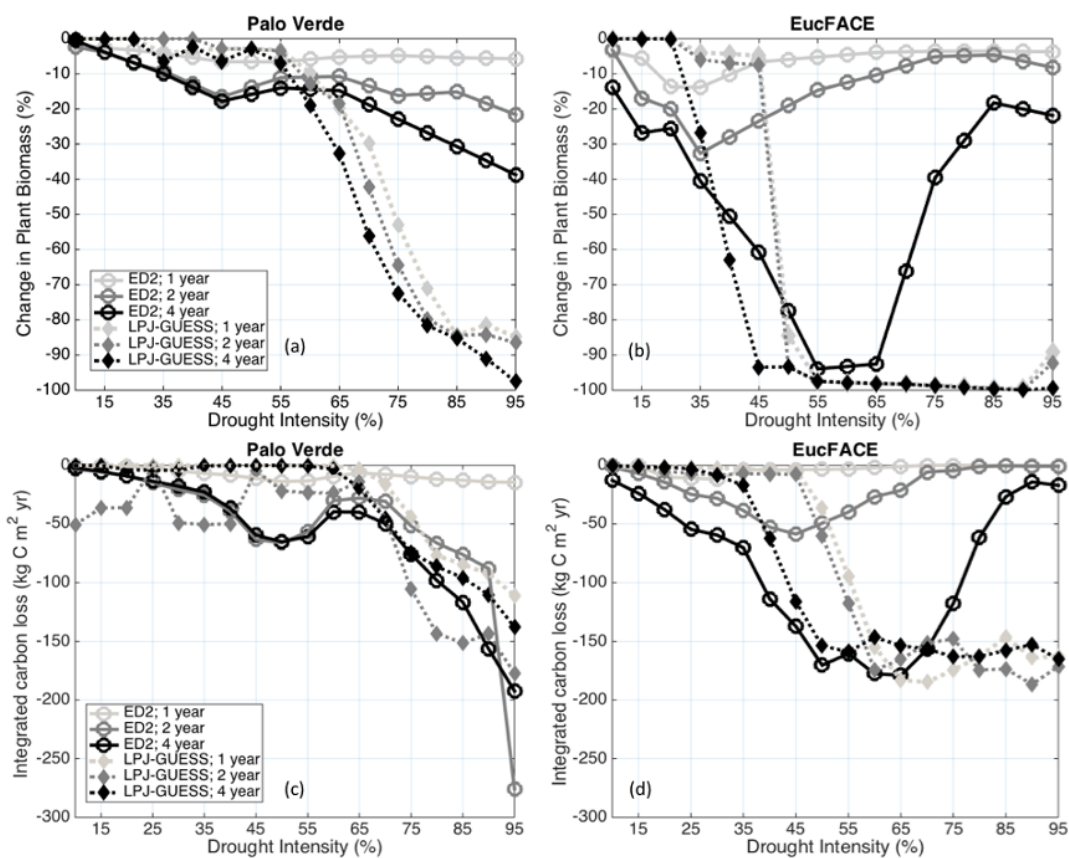


777

778 **Figure 1** Conceptual diagrams showing impacts of extreme droughts (unprecedented climate
 779 extremes, UCEs; i.e., record-breaking droughts) on plant C stocks. (a) **Conceptual response**
 780 **diagram**: potential loss in C stock as a function of increasing drought intensity (0-100%
 781 precipitation removal) and drought duration (1, 2 or 4 years of drought). In this example, an
 782 arbitrary threshold of 45% precipitation reduction and 4-year drought duration is assumed to
 783 correspond to a UCE. The “null hypothesis” (H0, top panel) is a linear response of C stocks to
 784 droughts. Alternative hypotheses include nonlinear and threshold responses to drought intensity
 785 (H1a), drought duration via different slope responses (H1b), and combined effects of both
 786 drought intensity and durations (H1c). (b) **Conceptualized UCE C loss diagram**: responses of
 787 forest C stocks to a large (grey) and small (black) UCE. “Integrated-C-loss” ($\text{kg C m}^{-2} \text{ yr}$)
 788 denotes the integral of the C loss over time and is calculated from the two arrows: the total loss
 789 in C (kg C m^{-2}) due to drought, and the time (yr) to recover 50% of the pre-drought C stock. (c)
 790 **Conceptualized UCE-climate C change diagram**: hypothetical response in terrestrial



791 “integrated-C-change” ($\text{kg C m}^{-2} \text{ yr}$) due to $e\text{CO}_2$ (blue line), rising temperature (red line),
792 interaction between $e\text{CO}_2$ and temperature (dashed purple), and combined interactions among
793 $e\text{CO}_2$, temperature, and UCEs of prolonged durations (green line), all relative to a reference
794 drought of normal duration with no warming (black line). Integrated-C-change denotes the
795 difference in integrated-C-loss (see panel b) between a scenario of changing climatic drivers and
796 the reference drought (control). (d) **Conceptual UCE amplification diagram:** hypothetical
797 amplified change in forest C stocks to $e\text{CO}_2$ and temperature relative to the pre-warming
798 historical past (based on Jump et al. (2017)). Change in C stock greater than zero indicates a
799 ‘structural overshoot’ (SO) due to favorable environmental conditions and/or recovery from an
800 extreme drought-heat event (EE). Hashed black areas indicate a structural overshoot due to
801 $e\text{CO}_2$, which occurs over the historical CO_2 levels (dashed blue line). Initially, an $e\text{CO}_2$ effect
802 leads to a larger increase in structural overshoot (due to CO_2 fertilization), driving more extreme
803 vegetation mortality (‘mortality overshoot’ - MO) relative to historical dieback events and thus a
804 greater decrease in C stock. Increased warming through time increasingly counteracts any CO_2
805 fertilization effect; while the amplitude of post-UCE C stock recoveries remains large, net C
806 stock values eventually decline (downward curvature) due to more pronounced loss in C stocks
807 (and greater ecosystem state change) from hotter UCEs.
808 SO = structural overshoot, MO = mortality overshoot, EE = historically extreme drought-heat
809 event, UCE = unprecedented climate extreme.
810



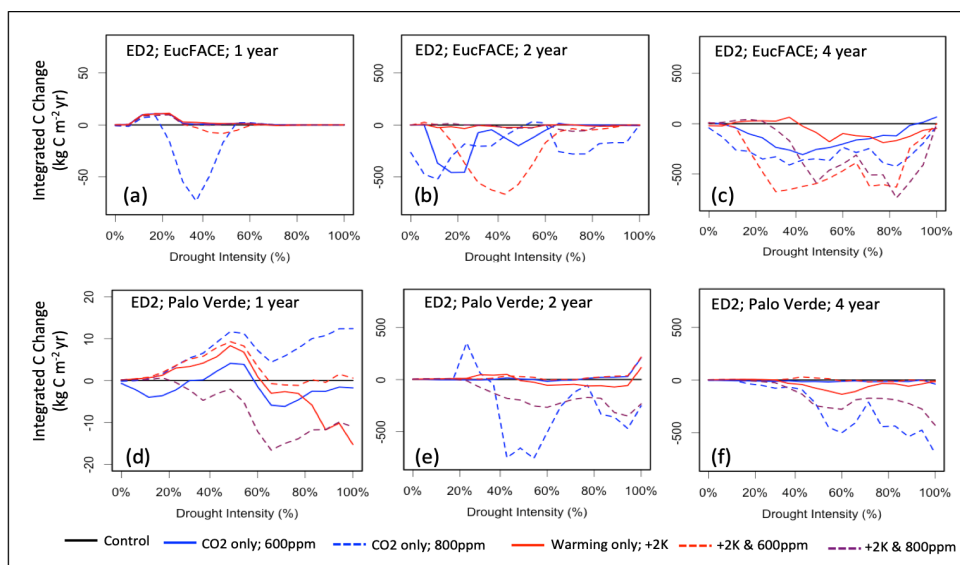
811

812 **Figure 2** Modeled change in biomass (%) at the end of drought periods of different lengths (1, 2,
813 and 4-year droughts) and intensities (up to 95% precipitation removed) at (a) Palo Verde, and (b)
814 EucFACE, for the ED2 and LPJ-GUESS models. Modeled integrated-C-loss (C reduction due to
815 extreme drought integrated over time until biomass recovers to 50% of the non-drought baseline
816 biomass) at (c) Palo Verde and (d) EucFACE.

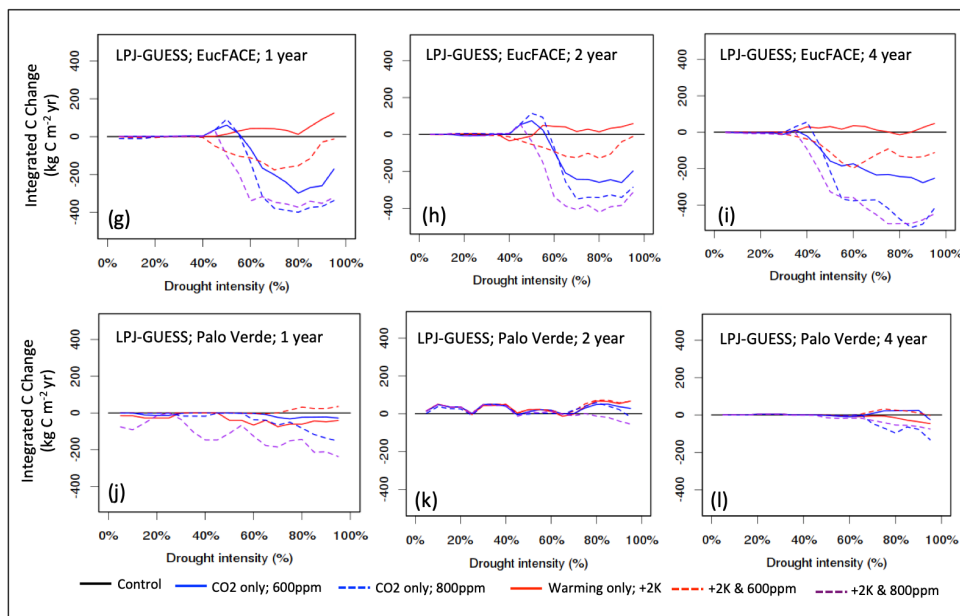
817



818



819



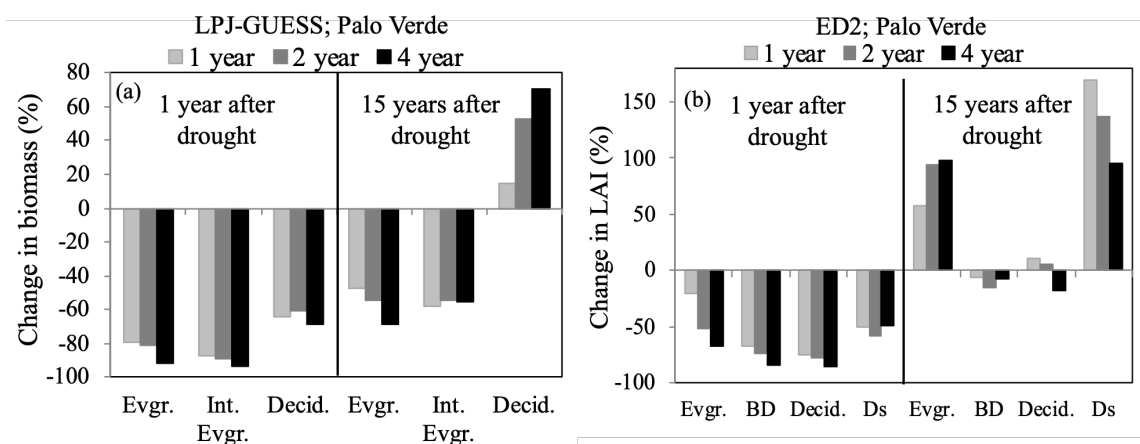
820 **Figure 3** Vegetation C response to interactions between drought intensity (0% to 100%
 821 precipitation reduction), drought durations (1, 2, 4-year droughts), and idealized scenarios of
 822 warming and eCO₂ compared to the reference simulation, simulated by two VDMs; ED2 (a-f)
 823 and LPJ-GUESS (g-l) at two sites (EucFACE and Palo Verde). The scenarios include a control
 824 (current temperature; 400 ppm atmospheric CO₂), two eCO₂ scenarios (600 ppm or 800 ppm),



825 elevated temperature (2 K above current), and a combination of eCO₂ (600 ppm or 800 ppm) and
826 higher temperature. Vegetation response is quantified as “integrated-C-change” (in kg C m⁻² yr;
827 Eq. 4), which is defined as the difference in integrated-C-losses due to drought between a given
828 scenario of change in climatic drivers and the control. Negative values for integrated-C-change
829 indicate that warming and/or eCO₂ leads to stronger C losses and/or longer recovery, while
830 positive values for integrated-C-change indicates a buffering effect.



831



832

833

834 **Figure 4** Percent change in community composition, represented by plant functional type (PFT),
 835 the year following three drought durations of UCEs (1, 2, and 4-year droughts and 90%
 836 precipitation removed) as well as 15 years after droughts, for the tropical Palo Verde site by (a)
 837 LPJ-GUESS reported in biomass change, and (b) ED2 reported in LAI change. Even though Ds
 838 had the strongest recovery, it should be noted it was the least abundant PFT at this site. Evgr. =
 839 evergreen, Int. Ever. = intermediate evergreen, Decid. = deciduous, BD = brevi-deciduous, Ds =
 840 deciduous stem-succulent. EucFACE data not shown because only one PFT present (evergreen
 841 tree).



842 References:

843

- 844 Adams, H.D., Guardiola-Claramonte, M., Barron-Gafford, G.A., Villegas, J.C., Breshears, D.D.,
845 Zou, C.B. et al.: Temperature sensitivity of drought-induced tree mortality portends
846 increased regional die-off under global-change-type drought, *PNAS*, 106, 7063-7066, 2009.
- 847 Adams, H.D., Barron-Gafford, G.A., Minor, R.L., Gardea, A.A., Bentley, L.P., Law, D.J. et al.:
848 Temperature response surfaces for mortality risk of tree species with future drought,
849 *Environ. Res. Lett.*, 12, 115014, 2017a.
- 850 Adams, H.D., Zeppel, M.J.B., Anderegg, W.R.L., Hartmann, H., Landhäusser, S.M., Tissue, D.T.
851 et al.: A multi-species synthesis of physiological mechanisms in drought-induced tree
852 mortality, *Nature Ecol. & Evol.*, 1, 1285-1291, 2017b.
- 853 Aguirre, BA, Hsieh, B, Watson, SJ, Wright, AJ.: The experimental manipulation of atmospheric
854 drought: Teasing out the role of microclimate in biodiversity experiments, *J. Ecol.*, 109,
855 1986– 1999, <https://doi.org/10.1111/1365-2745.13595>, 2021.
- 856 Ahlström, A., Schurgers, G., Arneth, A. & Smith, B.: Robustness and uncertainty in terrestrial
857 ecosystem carbon response to CMIP5 climate change projections, *Environ. Res. Lett.*, 7,
858 044008, 2012.
- 859 Ainsworth, E.A. & Long, S.P.: What have we learned from 15 years of free-air CO₂ enrichment
860 (FACE)? A meta-analytic review of the responses of photosynthesis, canopy properties and
861 plant production to rising CO₂, *New Phytol.*, 165, 351-372, 2005.
- 862 Allen, C.D., Breshears, D.D. & McDowell, N.G.: On underestimation of global vulnerability to
863 tree mortality and forest die-off from hotter drought in the Anthropocene, *Ecosphere*, 6,
864 art129, 2015.
- 865 Amiro, B.D., Barr, A.G., Barr, J.G., Black, T.A., Bracho, R., Brown, M. et al.: Ecosystem carbon
866 dioxide fluxes after disturbance in forests of North America, *J. Geophys. Res.*
867 *Biogeosciences*, 115, 2010.
- 868 Anderegg, W.R.L., Hicke, J.A., Fisher, R.A., Allen, C.D., Aukema, J., Bentz, B. et al.: Tree
869 mortality from drought, insects, and their interactions in a changing climate, *New Phytol.*,
870 208, 674-683, 2015.
- 871 Anderegg, W.R.L., Klein, T., Bartlett, M., Sack, L., Pellegrini, A.F.A., Choat, B. et al.: Meta-
872 analysis reveals that hydraulic traits explain cross-species patterns of drought-induced tree
873 mortality across the globe, *PNAS*, 113, 5024-5029, 2016a.
- 874 Anderegg, W.R.L., Martinez-Vilalta, J., Cailleret, M., Camarero, J.J., Ewers, B.E., Galbraith, D.
875 et al.: When a Tree Dies in the Forest: Scaling Climate-Driven Tree Mortality to Ecosystem
876 Water and Carbon Fluxes, *Ecosystems*, 19, 1133-1147, 2016b.
- 877 Anderegg, W.R.L., Konings, A.G., Trugman, A.T., Yu, K., Bowling, D.R., Gabbitas, R. et al.:
878 Hydraulic diversity of forests regulates ecosystem resilience during drought, *Nature*, 561,
879 538-541, 2018.
- 880 Asner, G.P., Brodrick, P.G., Anderson, C.B., Vaughn, N., Knapp, D.E. & Martin, R.E.:
881 Progressive forest canopy water loss during the 2012–2015 California drought. *PNAS*, 113,
882 E249-E255, 2016.
- 883 Arora, V.K., Katavouta, A., Williams, R.G., Jones, C.D., Brovkin, V., Friedlingstein, P., et
884 al.: Carbon-concentration and carbon-climate feedbacks in CMIP6 models and their
885 comparison to CMIP5 models, *Biogeosciences*, 17, 4173–4222, 2020.



- 886 Bai, Y., Wu, J., Xing, Q., Pan, Q., Huang, J., Yang, D. et al.: PRIMARY PRODUCTION AND
887 RAIN USE EFFICIENCY ACROSS A PRECIPITATION GRADIENT ON THE
888 MONGOLIA PLATEAU, *Ecology*, 89, 2140-2153, 2008.
- 889 Beier, C., Beierkuhnlein, C., Wohlgemuth, T., Penuelas, J., Emmett, B., Körner, C. et al.:
890 Precipitation manipulation experiments – challenges and recommendations for the future,
891 *Ecol. Lett.*, 15, 899-911, 2012.
- 892 Bennett, A.C., McDowell, N.G., Allen, C.D. & Anderson-Teixeira, K.J.: Larger trees suffer most
893 during drought in forests worldwide, *Nature Plants*, 1, 15139, 2015.
- 894 Biederman, J.A., Meixner, T., Harpold, A.A., Reed, D.E., Gutmann, E.D., Gaun, J.A. et al.:
895 Riparian zones attenuate nitrogen loss following bark beetle-induced lodgepole pine
896 mortality, *J. Geophys. Res. Biogeosciences*, 121, 933-948, 2016.
- 897 Biederman, J.A., Somor, A.J., Harpold, A.A., Gutmann, E.D., Breshears, D.D., Troch, P.A. et al.:
898 Recent tree die-off has little effect on streamflow in contrast to expected increases from
899 historical studies, *Water Resources Res.*, 51, 9775-9789, 2015.
- 900 Borchert, R., Rivera, G. & Hagnauer, W.: Modification of Vegetative Phenology in a Tropical
901 Semi-deciduous Forest by Abnormal Drought and Rain, *Biotropica*, 34, 27-39, 2002.
- 902 Brando, P.M., Paolucci, L., Ummenhofer, C.C., Ordway, E.M., Hartmann, H., Cattau, M.E.,
903 Rattis, L., Medjibe, V., Coe, M.T., Balch, J.: Droughts, Wildfires, and Forest Carbon
904 Cycling: A Pantropical Synthesis, *Annual Review of Earth and Planetary Sciences*, 47, 555-
905 581, 2019.
- 906 Breshears, D.D., Myers, O.B., Meyer, C.W., Barnes, F.J., Zou, C.B., Allen, C.D. et al.: Tree die-
907 off in response to global change-type drought: mortality insights from a decade of plant
908 water potential measurements, *Front. Ecol. Environ.*, 7, 185-189, 2009.
- 909 Brodrigg, T.J., Bowman, D.J.M.S., Nichols, S., Delzon, S. & Burlett, R.: Xylem function and
910 growth rate interact to determine recovery rates after exposure to extreme water deficit, *New
911 Phytol.*, 188, 533-542, 2010.
- 912 Carreño-Rocabado, G., Peña-Claros, M., Bongers, F., Alarcón, A., Licona, J.-C. & Poorter, L.:
913 Effects of disturbance intensity on species and functional diversity in a tropical forest, *J.
914 Ecology*, 100, 1453-1463, 2012.
- 915 Chapman, T.B., Veblen, T.T. & Schoennagel, T.: Spatiotemporal patterns of mountain pine beetle
916 activity in the southern Rocky Mountains, *Ecology*, 93, 2175-2185, 2012.
- 917 Chiang, F., Mazdiyasn, O. & AghaKouchak, A.: Evidence of anthropogenic impacts on global
918 drought frequency, duration, and intensity, *Nat Commun.*, 12, 2754,
919 <https://doi.org/10.1038/s41467-021-22314-w>, 2021.
- 920 Choat, B., Brodrigg, T.J., Brodersen, C.R., Duursma, R.A., López, R. & Medlyn, B.E.: Triggers
921 of tree mortality under drought, *Nature*, 558, 531-539, 2018.
- 922 Choat, B., Jansen, S., Brodrigg, T.J., Cochard, H., Delzon, S., Bhaskar, R. et al.: Global
923 convergence in the vulnerability of forests to drought, *Nature*, 491, 752-755, 2012.
- 924 Christoffersen, B.O., Gloor, M., Fauset, S., Fyllas, N.M., Galbraith, D.R., Baker, T.R. et al.:
925 Linking hydraulic traits to tropical forest function in a size-structured and trait-driven model
926 (TFS v.1-Hydro), *Geosci. Model Dev. Discuss.*, 2016, 1-60, 2016.
- 927 Ciais, P., Reichstein, M., Viovy, N., Granier, A., Ogée, J., Allard, V. et al.: Europe-wide
928 reduction in primary productivity caused by the heat and drought in 2003, *Nature*, 437, 529,
929 2005.
- 930 Ciais, P., Sabine, C., Bala, G., Bopp, L., Brovkin, V., Canadell, J., et al.: Carbon and other
931 biogeochemical cycles. In: *Climate Change 2013: The Physical Science Basis*.



- 932 Contribution of Working Group I to the Fifth Assessment Report of the
933 Intergovernmental Panel on Climate Change (eds. Stocker, T.F., Qin, D., Plattner, G.-K.,
934 Tignor, M., Allen, S.K., Boschung, J., et al.), Cambridge University Press, Cambridge,
935 United Kingdom and New York, NY, USA, pp. 465–570, 2013.
- 936 Clark, K.L., Skowronski, N. & Hom, J.: Invasive insects impact forest carbon dynamics, *Glob.*
937 *Change Biol.*, 16, 88-101, 2010.
- 938 Coley, P., Massa, M., Lovelock, C., Winter, K.: Effects of elevated CO₂ on foliar chemistry of
939 saplings of nine species of tropical tree, *Oecologia*, 2002.
- 940 Creeden, E.P., Hicke, J.A. & Buotte, P.C.: Climate, weather, and recent mountain pine beetle
941 outbreaks in the western United States, *Forest Ecol. Manag.*, 312, 239-251, 2014.
- 942 D'Amato, A.W., Bradford, J.B., Fraver, S. & Palik, B.J.: Effects of thinning on drought
943 vulnerability and climate response in north temperate forest ecosystems, *Eco. Applications*,
944 23, 1735-1742, 2013.
- 945 da Costa, A.C.L., Galbraith, D., Almeida, S., Portela, B.T.T., da Costa, M., de Athaydes Silva
946 Junior, J. et al., Effect of 7 yr of experimental drought on vegetation dynamics and biomass
947 storage of an eastern Amazonian rainforest, *New Phytol.*, 187, 579-591, 2010.
- 948 De Kauwe, M.G., Medlyn, B.E., Zaehle, S., Walker, A.P., Dietze, M.C., Wang, Y.-P. et al.:
949 Where does the carbon go? A model-data intercomparison of vegetation carbon allocation
950 and turnover processes at two temperate forest free-air CO₂ enrichment sites, *New Phytol.*,
951 203, 883-899, 2014.
- 952 Dietze, M.C. & Matthes, J.H.: A general ecophysiological framework for modelling the impact of
953 pests and pathogens on forest ecosystems, *Ecol. Lett.*, 17, 1418-1426, 2014.
- 954 Döscher, R., Acosta, M., et al.: The EC-Earth3 Earth System Model for the Climate Model
955 Intercomparison Project 6, *Geosci. Model Dev. Discuss.* [preprint],
956 <https://doi.org/10.5194/gmd-2020-446>, in revision, 2022.
- 957 Dreesen, F.E., De Boeck, H.J., Janssens, I.A. & Nijs, I.: Do successive climate extremes weaken
958 the resistance of plant communities? An experimental study using plant assemblages,
959 *Biogeosciences*, 11, 109-121, 2014.
- 960 Eamus, D., Boulain, N., Cleverly, J. & Breshears, D.D.: Global change-type drought-induced tree
961 mortality: vapor pressure deficit is more important than temperature per se in causing
962 decline in tree health, *Ecol. Evol.*, 3, 2711-2729, 2013.
- 963 Ellsworth, David S., Anderson, Ian C., Crous, Kristine Y., Cooke, J., Drake, John E., Gherlenda,
964 Andrew N. et al.: Elevated CO₂ does not increase eucalypt forest productivity on a low-
965 phosphorus soil, *Nature Climate Change*, 7, 279, 2017.
- 966 ENQUIST, B.J. & ENQUIST, C.A.F.: Long-term change within a Neotropical forest: assessing
967 differential functional and floristic responses to disturbance and drought, *Glob. Change*
968 *Biol.*, 17, 1408-1424, 2011.
- 969 Esquivel-Muelbert, A., Baker, T.R., Dexter, K.G., Lewis, S.L., Brienen, R.J.W., Feldpausch, T.R.
970 et al.: Compositional response of Amazon forests to climate change, *Glob. Change Biol.*, 25,
971 39-56, 2019.
- 972 Eziz, A., Yan, Z., Tian, D., Han, W., Tang, Z. & Fang, J.: Drought effect on plant biomass
973 allocation: A meta-analysis, *Ecol. Evol.*, 7, 11002-11010, 2017.
- 974 Feldpausch, T.R., Phillips, O.L., Brienen, R.J.W., Gloor, E., Lloyd, J., Lopez-Gonzalez, G. et al.:
975 Amazon forest response to repeated droughts, *Global Biogeochemical Cycles*, 30, 964-982,
976 2016.



- 977 Fisher, R.A., Muszala, S., Versteinstein, M., Lawrence, P., Xu, C., McDowell, N.G. et al.: Taking
978 off the training wheels: the properties of a dynamic vegetation model without climate
979 envelopes, *CLM4.5(ED)*, *Geosci. Model Dev.*, 8, 3593-3619, 2015.
- 980 Fisher, R.A., Koven, C.D., Anderegg, W.R.L., Christoffersen, B.O., Dietze, M.C., Farrior, C.E. et
981 al.: Vegetation demographics in Earth System Models: A review of progress and priorities,
982 *Glob. Change Biol.*, 24, 35-54, 2018.
- 983 Fisher, R. A., and Koven, C. D.: Perspectives on the future of land surface models and the
984 challenges of representing complex terrestrial systems, *JAMES*, 12,
985 e2018MS001453, <https://doi.org/10.1029/2018MS001453>, 2020.
- 986 Fleischer, K., Rammig, A., De Kauwe, M.G., Walker, A.P., Domingues, T.F., Fuchslueger, L. et
987 al.: Amazon forest response to CO₂ fertilization dependent on plant phosphorus acquisition,
988 *Nature Geoscience*, 12, 736-741, 2019.
- 989 Frank, D., Reichstein, M., Bahn, M., Thonicke, K., Frank, D., Mahecha, M.D. et al.: Effects of
990 climate extremes on the terrestrial carbon cycle: concepts, processes and potential future
991 impacts, *Glob. Change Biol.*, 21, 2861-2880, 2015.
- 992 Friend, A.D., Lucht, W., Rademacher, T.T., Keribin, R., Betts, R., Cadule, P. et al.: Carbon
993 residence time dominates uncertainty in terrestrial vegetation responses to future climate
994 and atmospheric CO₂, *PNAS*, 111, 3280-3285, 2014.
- 995 Gerten, D., LUO, Y., Le MAIRE, G., PARTON, W.J., KEOUGH, C., WENG, E. et al.: Modelled
996 effects of precipitation on ecosystem carbon and water dynamics in different climatic zones,
997 *Glob. Change Biol.*, 14, 2365-2379, 2008.
- 998 Goulden, M.L. & Bales, R.C.: California forest die-off linked to multi-year deep soil drying in
999 2012–2015 drought, *Nature Geoscience*, 12, 632-637, 2019.
- 1000 Gray, S.B., Dermody, O., Klein, S.P., Locke, A.M., McGrath, J.M., Paul, R.E. et al.: Intensifying
1001 drought eliminates the expected benefits of elevated carbon dioxide for soybean, *Nature*
1002 *Plants*, 2, 16132, 2016.
- 1003 Greenwood, S., Ruiz-Benito, P., Martínez-Vilalta, J., Lloret, F., Kitzberger, T., Allen, C.D. et al.:
1004 Tree mortality across biomes is promoted by drought intensity, lower wood density and
1005 higher specific leaf area, *Ecol. Lett.*, 20, 539-553, 2017.
- 1006 Griffin, D. & Anchukaitis, K.J.: How unusual is the 2012–2014 California drought? *Geophys.*
1007 *Res. Lett.*, 41, 9017-9023, 2014.
- 1008 Hickler, T., Smith, B., Sykes, M.T., Davis, M.B., Sugita, S. & Walker, K.: USING A
1009 GENERALIZED VEGETATION MODEL TO SIMULATE VEGETATION DYNAMICS
1010 IN NORTHEASTERN USA, *Ecology*, 85, 519-530, 2004.
- 1011 Holm, J. A., Knox, R. G., Zhu, Q., Fisher, R. A., Koven, C. D., Nogueira Lima, A. J., et al.: The
1012 central Amazon biomass sink under current and future atmospheric CO₂: Predictions from
1013 big-leaf and demographic vegetation models, *J. Geophys. Res. Biogeosciences*, 125,
1014 e2019JG005500. <https://doi.org/10.1029/2019JG005500>, 2020.
- 1015 Hovenden, M.J., Newton, P.C.D. & Wills, K.E.: Seasonal not annual rainfall determines grassland
1016 biomass response to carbon dioxide, *Nature*, 511, 583, 2014.
- 1017 Hubbard, R.M., Rhoades, C.C., Elder, K. & Negron, J.: Changes in transpiration and foliage
1018 growth in lodgepole pine trees following mountain pine beetle attack and mechanical
1019 girdling, *Forest Ecol. Manag.*, 289, 312-317, 2013.
- 1020 IPCC: Managing the Risks of Extreme Events and Disasters to Advance Climate Change
1021 Adaptation. A Special Report of Working Groups I and II of the Intergovernmental Panel on
1022 Climate Change. (ed. Field, CB, V. Barros, T.F. Stocker, D. Qin, D.J. Dokken, K.L. Ebi,



- 1023 M.D. Mastrandrea, K.J. Mach, G.-K. Plattner, S.K. Allen, M. Tignor, and P.M. Midgley
1024 Cambridge, UK, and New York, NY, USA, p. 582 pp, 2012.
- 1025 IPCC: Climate Change 2021: The Physical Science Basis. Contribution of Working Group I to the
1026 Sixth Assessment Report of the Intergovernmental Panel on Climate Change [Masson-
1027 Delmotte, V., P. Zhai, A. Pirani, S.L. Connors, C. Péan, S. Berger, N. Caud, Y. Chen, L.
1028 Goldfarb, M.I. Gomis, M. Huang, K. Leitzell, E. Lonnoy, J.B.R. Matthews, T.K. Maycock,
1029 T. Waterfield, O. Yelekçi, R. Yu, and B. Zhou (eds.)]. Cambridge University Press. In
1030 Press, 2021.
- 1031 Jiang, M., Medlyn, B.E., Drake, J.E., Duursma, R.A., Anderson, I.C., Barton, C.V.M., Boer,
1032 M.B., Carrillo, Y., Castañeda-Gómez, L., Collins, L., et al.: The fate of carbon in a mature
1033 forest under carbon dioxide enrichment, *Nature*, 580, 227-231,
1034 <https://doi.org/10.1038/s41586-020-2128-9>, 2020.
- 1035 Joslin, J.D., Wolfe, M.H. & Hanson, P.J.: Effects of altered water regimes on forest root systems,
1036 *New Phytol.*, 147, 117-129, 2000.
- 1037 Jump, A.S., Ruiz-Benito, P., Greenwood, S., Allen, C.D., Kitzberger, T., Fensham, R. et al.:
1038 Structural overshoot of tree growth with climate variability and the global spectrum of
1039 drought-induced forest dieback, *Glob. Change Biol.*, 23, 3742-3757, 2017.
- 1040 Kannenberg, S.A., Schwalm, C.R. and Anderegg, W.R.L.: Ghosts of the past: how drought legacy
1041 effects shape forest functioning and carbon cycling, *Ecol. Lett.*, 23: 891-901,
1042 <https://doi.org/10.1111/ele.13485>, 2020.
- 1043 Kattge, J., DÍAZ, S., LAVOREL, S., PRENTICE, I.C., LEADLEY, P., BÖNISCH, G. et al.: TRY
1044 – a global database of plant traits, *Global Change Biol*, 17, 2905-2935, 2011.
- 1045 Kayler, Z.E., De Boeck, H.J., Fatichi, S., Grünzweig, J.M., Merbold, L., Beier, C. et al.:
1046 Experiments to confront the environmental extremes of climate change, *Front. Ecol.*
1047 *Environ.*, 13, 219-225, 2015.
- 1048 Keenan, T.F., Hollinger, D.Y., Bohrer, G., Dragoni, D., Munger, J.W., Schmid, H.P. et al.:
1049 Increase in forest water-use efficiency as atmospheric carbon dioxide concentrations rise,
1050 *Nature*, 499, 324-327, 2013.
- 1051 Kennedy, D., Swenson, S., Oleson, K. W., Lawrence, D. M., Fisher, R., Lola da Costa, A. C., &
1052 Gentine, P.: Implementing plant hydraulics in the Community Land Model, version 5,
1053 *JAMES*, 11, 485– 513. <https://doi.org/10.1029/2018MS001500>, 2019.
- 1054 Liu, Y., Parolari, A.J., Kumar, M., Huang, C.-W., Katul, G.G. & Porporato, A.: Increasing
1055 atmospheric humidity and CO₂ concentration alleviate forest mortality risk, *PNAS*, 114,
1056 9918-9923, 2017.
- 1057 Lloret, F., Escudero, A., Iriondo, J.M., Martínez-Vilalta, J. & Valladares, F.: Extreme climatic
1058 events and vegetation: the role of stabilizing processes, *Glob. Change Biol.*, 18, 797-805,
1059 2012.
- 1060 Luo, Y., Gerten, D., Le Maire, G., Parton, W.J., Weng, E., Zhou, X. et al.: Modeled interactive
1061 effects of precipitation, temperature, and [CO₂] on ecosystem carbon and water dynamics in
1062 different climatic zones, *Glob. Change Biol.*, 14, 1986-1999, 2008.
- 1063 Luo, Y.Q., Randerson, J.T., Abramowitz, G., Bacour, C., Blyth, E., Carvalhais, N. et al.: A
1064 framework for benchmarking land models, *Biogeosciences*, 9, 3857-3874, 2012.
- 1065 Luo, Y., Jiang, L., Niu, S., Zhou, X.: Nonlinear responses of land ecosystems to variation in
1066 precipitation, *New Phytol.*, 214, 5–7, 2017.



- 1067 MacGillivray, C.W., Grime, J.P. & The Integrated Screening Programme, T.: Testing Predictions
1068 of the Resistance and Resilience of Vegetation Subjected to Extreme Events, *Funct. Ecol.*, 9,
1069 640-649, 1995.
- 1070 Markewitz, D., Devine, S., Davidson, E.A., Brando, P. & Nepstad, D.C.: Soil moisture depletion
1071 under simulated drought in the Amazon: impacts on deep root uptake, *New Phytol.*, 187,
1072 592-607, 2010.
- 1073 Matusick, G., Ruthrof, K.X., Brouwers, N.C., Dell, B. & Hardy, G.S.J.: Sudden forest canopy
1074 collapse corresponding with extreme drought and heat in a mediterranean-type eucalypt
1075 forest in southwestern Australia, *European J. Forest Res.*, 132, 497-510, 2013.
- 1076 Matusick, G., Ruthrof, K.X., Fontaine, J.B. & Hardy, G.E.S.J.: Eucalyptus forest shows low
1077 structural resistance and resilience to climate change-type drought, *J. Vegetation Science*,
1078 27, 493-503, 2016.
- 1079 McCarthy, M.C. & Enquist, B.J.: Consistency between an allometric approach and optimal
1080 partitioning theory in global patterns of plant biomass allocation, *Funct. Ecol.*, 21, 713-720,
1081 2007.
- 1082 McDowell, N., Pockman, W.T., Allen, C.D., Breshears, D.D., Cobb, N., Kolb, T. et al.:
1083 Mechanisms of plant survival and mortality during drought: why do some plants survive
1084 while others succumb to drought? *New Phytol.*, 178, 719-739, 2008.
- 1085 McDowell, N.G., Adams, H.D., Bailey, J.D., Hess, M. & Kolb, T.E.: Homeostatic Maintenance
1086 Of Ponderosa Pine Gas Exchange In Response To Stand Density Changes, *Ecological
1087 Applications*, 16, 1164-1182, 2006.
- 1088 McDowell, N.G. & Allen, C.D.: Darcy's law predicts widespread forest mortality under climate
1089 warming, *Nature Climate Change*, 5, 669-672, 2015.
- 1090 McDowell, N.G., Beerling, D.J., Breshears, D.D., Fisher, R.A., Raffa, K.F. & Stitt, M.: The
1091 interdependence of mechanisms underlying climate-driven vegetation mortality, *Trends in
1092 Ecol. & Evolution*, 26, 523-532, 2011.
- 1093 McDowell, N.G., Fisher, R.A., Xu, C., Domec, J.C., Hölttä, T., Mackay, D.S. et al.: Evaluating
1094 theories of drought-induced vegetation mortality using a multimodel–experiment
1095 framework, *New Phytol.*, 200, 304-321, 2013.
- 1096 Medvigy, D., Clark, K.L., Skowronski, N.S. & Schäfer, K.V.R.: Simulated impacts of insect
1097 defoliation on forest carbon dynamics, *Environ. Res. Lett.*, 7, 045703, 2012.
- 1098 Medvigy, D. & Moorcroft, P.R.: Predicting ecosystem dynamics at regional scales: an evaluation
1099 of a terrestrial biosphere model for the forests of northeastern North America, *Philosophical
1100 Transactions of the Royal Society B: Biological Sciences*, 367, 222-235, 2012.
- 1101 Medvigy, D., Wofsy, S., Munger, J., Hollinger, D. & Moorcroft, P.: Mechanistic scaling of
1102 ecosystem function and dynamics in space and time: Ecosystem Demography model version
1103 2, *J. Geophys. Res. Biogeosciences*, 114, 2009.
- 1104 Meir, P., Wood, T.E., Galbraith, D.R., Brando, P.M., Da Costa, A.C.L., Rowland, L. et al.:
1105 Threshold Responses to Soil Moisture Deficit by Trees and Soil in Tropical Rain Forests:
1106 Insights from Field Experiments, *BioScience*, 65, 882-892, 2015.
- 1107 Montané, F., Fox, A.M., Arellano, A.F., MacBean, N., Alexander, M.R., Dye, A. et al.:
1108 Evaluating the effect of alternative carbon allocation schemes in a land surface model
1109 (CLM4.5) on carbon fluxes, pools, and turnover in temperate forests, *Geosci. Model Dev.*,
1110 10, 3499-3517, 2017.



- 1111 Muldavin, E.H., Moore, D.I., Collins, S.L., Wetherill, K.R. & Lightfoot, D.C.: Aboveground net
1112 primary production dynamics in a northern Chihuahuan Desert ecosystem, *Oecologia*, 155,
1113 123-132, 2008.
- 1114 Myers, J.A. & Kitajima, K.: Carbohydrate storage enhances seedling shade and stress tolerance in
1115 a neotropical forest, *J. Ecology*, 95, 383-395, 2007.
- 1116 Niklas, K. J.: The scaling of plant height: A comparison among major plant clades and anatomical
1117 grades, *Annals of Botany*, 72, 165–172, <https://doi.org/10.1006/anbo.1993.1095>, 1993.
- 1118 Norby, R.J., DeLucia, E.H., Gielen, B., Calfapietra, C., Giardina, C.P., King, J.S. et al.: Forest
1119 response to elevated CO₂ is conserved across a broad range of productivity, *PNAS*, 102,
1120 18052-18056, 2005.
- 1121 O'Brien, M.J., Leuzinger, S., Philipson, C.D., Tay, J. & Hector, A.: Drought survival of tropical
1122 tree seedlings enhanced by non-structural carbohydrate levels, *Nature Climate Change*, 4,
1123 710, 2014.
- 1124 Obermeier, W.A., Lehnert, L.W., Kammann, C.I., Müller, C., Grünhage, L., Luterbacher, J. et al.:
1125 Reduced CO₂ fertilization effect in temperate C₃ grasslands under more extreme weather
1126 conditions, *Nature Climate Change*, 7, 137, 2016.
- 1127 Palace, M., Keller, M. & Silva, H.: NECROMASS PRODUCTION: STUDIES IN
1128 UNDISTURBED AND LOGGED AMAZON FORESTS, *Ecological Applications*, 18, 873-
1129 884, 2008.
- 1130 Phillips, O.L., Aragão, L.E.O.C., Lewis, S.L., Fisher, J.B., Lloyd, J., López-González, G. et al.:
1131 Drought Sensitivity of the Amazon Rainforest, *Science*, 323, 1344-1347, 2009.
- 1132 Phillips, O.L., van der Heijden, G., Lewis, S.L., López-González, G., Aragão, L.E.O.C., Lloyd, J.
1133 et al.: Drought–mortality relationships for tropical forests, *New Phytol.*, 187, 631-646, 2010.
- 1134 Pilon, C.E., Côté, B. & Fyles, J.W.: Effect of an artificially induced drought on leaf peroxidase
1135 activity, mineral nutrition and growth of sugar maple, *Plant and Soil*, 179, 151-158, 1996.
- 1136 Potter, C., Klooster, S., Hiatt, C., Genovese, V. & Castilla-Rubio, J.C.: Changes in the carbon
1137 cycle of Amazon ecosystems during the 2010 drought, *Environ. Res. Lett.*, 6, 034024, 2011.
- 1138 Powell, T.L., Galbraith, D.R., Christoffersen, B.O., Harper, A., Imbuzeiro, H.M.A., Rowland, L.
1139 et al.: Confronting model predictions of carbon fluxes with measurements of Amazon
1140 forests subjected to experimental drought, *New Phytol.*, 200, 350-365, 2013.
- 1141 Powell, T.L., Koven, C.D., Johnson, D.J., Faybishenko, B., Fisher, R.A., Knox, Ryan G. et al.:
1142 Variation in hydroclimate sustains tropical forest biomass and promotes functional diversity,
1143 *New Phytol.*, 219, 932-946, 2018.
- 1144 Powers, J.S., Becknell, J.M., Irving, J. & Pérez-Aviles, D.: Diversity and structure of regenerating
1145 tropical dry forests in Costa Rica: Geographic patterns and environmental drivers, *Forest
1146 Ecol. Manag.*, 258, 959-970, 2009.
- 1147 Powers, J.S. & Pérez-Aviles, D.: Edaphic Factors are a More Important Control on Surface Fine
1148 Roots than Stand Age in Secondary Tropical Dry Forests, *Biotropica*, 45, 1-9, 2013.
- 1149 Powers, JS, Vargas G., G, Brodribb, TJ, et al.: A catastrophic tropical drought kills hydraulically
1150 vulnerable tree species, *Glob. Change Biol.* 2020; 26: 3122– 3133,
1151 <https://doi.org/10.1111/gcb.15037>, 2020.
- 1152 Rapparini, F. & Peñuelas, J.: Mycorrhizal Fungi to Alleviate Drought Stress on Plant Growth. In:
1153 Use of Microbes for the Alleviation of Soil Stresses, Volume 1 (ed. Miransari, M), Springer
1154 New York New York, NY, pp. 21-42, 2014.
- 1155 Reich, P.B., Hobbie, S.E. & Lee, T.D.: Plant growth enhancement by elevated CO₂ eliminated by
1156 joint water and nitrogen limitation, *Nature Geoscience*, 7, 920, 2014.



- 1157 Reich, P.B., Wright, I.J. & Lusk, C.H.: PREDICTING LEAF PHYSIOLOGY FROM SIMPLE
1158 PLANT AND CLIMATE ATTRIBUTES: A GLOBAL GLOPNET ANALYSIS, *Ecological*
1159 *Applications*, 17, 1982-1988, 2007.
- 1160 Reichstein, M., Bahn, M., Ciais, P., Frank, D., Mahecha, M.D., Seneviratne, S.I. et al.: Climate
1161 extremes and the carbon cycle, *Nature*, 500, 287-295, 2013.
- 1162 Reyes, J.J., Tague, C.L., Evans, R.D. & Adam, J.C.: Assessing the Impact of Parameter
1163 Uncertainty on Modeling Grass Biomass Using a Hybrid Carbon Allocation Strategy, 9,
1164 2968-2992, 2017.
- 1165 Richardson, A.D., Carbone, M.S., Keenan, T.F., Czimczik, C.I., Hollinger, D.Y., Murakami, P. et
1166 al.: Seasonal dynamics and age of stemwood nonstructural carbohydrates in temperate forest
1167 trees, *New Phytol.*, 197, 850-861, 2013.
- 1168 Rowland, L., da Costa, A.C.L., Galbraith, D.R., Oliveira, R.S., Binks, O.J., Oliveira, A.A.R. et
1169 al.: Death from drought in tropical forests is triggered by hydraulics not carbon starvation,
1170 *Nature*, 528, 119, 2015.
- 1171 Roy, J., Picon-Cochard, C., Augusti, A., Benot, M.-L., Thiery, L., Darsonville, O. et al.: Elevated
1172 CO₂ maintains grassland net carbon uptake under a future heat and drought extreme, *PNAS*,
1173 113, 6224-6229, 2016.
- 1174 Ruppert, J.C., Harmony, K., Henkin, Z., Snyman, H.A., Sternberg, M., Willms, W. et al.:
1175 Quantifying drylands' drought resistance and recovery: the importance of drought intensity,
1176 dominant life history and grazing regime, *Glob. Change Biol.*, 21, 1258-1270, 2015.
- 1177 Rustad, L.E.: The response of terrestrial ecosystems to global climate change: Towards an
1178 integrated approach, *Science of The Total Environ.*, 404, 222-235, 2008.
- 1179 Ruthrof, K.X., Breshears, D.D., Fontaine, J.B., Froend, R.H., Matusick, G., Kala, J. et al.:
1180 Subcontinental heat wave triggers terrestrial and marine, multi-taxa responses, *Scientific*
1181 *Reports*, 8, 13094, 2018.
- 1182 Scheiter, S., Langan, L. & Higgins, S.I.: Next-generation dynamic global vegetation models:
1183 learning from community ecology, *New Phytol.*, 198, 957-969, 2013.
- 1184 Schenk, H.J. & Jackson, R.B.: Mapping the global distribution of deep roots in relation to climate
1185 and soil characteristics, *Geoderma*, 126, 129-140, 2005.
- 1186 Schwalm, C.R., Anderegg, W.R.L., Michalak, A.M., Fisher, J.B., Biondi, F., Koch, G. et al.:
1187 Global patterns of drought recovery, *Nature*, 548, 202, 2017.
- 1188 Seneviratne, S.I., X. Zhang, M. Adnan, W. Badi, C. Dereczynski, A. Di Luca, S. Ghosh, I.
1189 Iskandar, J. Kossin, S. Lewis, F. Otto, I. Pinto, M. Satoh, S.M. Vicente-Serrano, M. Wehner,
1190 and B. Zhou, 2021: Weather and Climate Extreme Events in a Changing Climate. In
1191 *Climate Change 2021: The Physical Science Basis. Contribution of Working Group I to the*
1192 *Sixth Assessment Report of the Intergovernmental Panel on Climate Change*
1193 [MassonDelmotte, V., P. Zhai, A. Pirani, S.L. Connors, C. Péan, S. Berger, N. Caud, Y.
1194 Chen, L. Goldfarb, M.I. Gomis, M. Huang, K. Leitzell, E. Lonnoy, J.B.R. Matthews, T.K.
1195 Maycock, T. Waterfield, O. Yelekçi, R. Yu, and B. Zhou (eds.)], Cambridge University
1196 Press, In Press.
- 1197 Settele, J., Scholes, R., Betts, R., Bunn, S.E., Leadley, P., Nepstad, D., Overpeck, J.T., and
1198 Taboada, M.A.: Terrestrial and inland water systems. In: *Climate Change 2014: Impacts,*
1199 *Adaptation, and Vulnerability. Part A: Global and Sectoral Aspects. Contribution of*
1200 *Working Group II to the Fifth Assessment Report of the Intergovernmental Panel on*
1201 *Climate Change*, Cambridge University Press Cambridge, United Kingdom and New York,
1202 NY, USA, pp. 271-359, 2014.



- 1203 Sheffield, J., Goteti, G. & Wood, E.F.: Development of a 50-Year High-Resolution Global
1204 Dataset of Meteorological Forcings for Land Surface Modeling, *J. Climate*, 19, 3088-3111,
1205 2006.
- 1206 Shiels, A.B., Zimmerman, J.K., García-Montiel, D.C., Jonckheere, I., Holm, J., Horton, D. et al.:
1207 Plant responses to simulated hurricane impacts in a subtropical wet forest, Puerto Rico, *J.*
1208 *Ecology*, 98, 659-673, 2010.
- 1209 Sippel, S., Zscheischler, J. & Reichstein, M.: Ecosystem impacts of climate extremes crucially
1210 depend on the timing, *PNAS*, 113, 5768-5770, 2016.
- 1211 Sitch, S., HUNTINGFORD, C., GEDNEY, N., LEVY, P.E., LOMAS, M., PIAO, S.L. et al.:
1212 Evaluation of the terrestrial carbon cycle, future plant geography and climate-carbon cycle
1213 feedbacks using five Dynamic Global Vegetation Models (DGVMs), *Glob. Change Biol.*,
1214 14, 2015-2039, 2008.
- 1215 Skelton, R.P., West, A.G. & Dawson, T.E.: Predicting plant vulnerability to drought in biodiverse
1216 regions using functional traits, *PNAS*, 112, 5744-5749, 2015.
- 1217 Smith, B., Prentice, I.C. & Sykes, M.T.: Representation of vegetation dynamics in the modelling
1218 of terrestrial ecosystems: comparing two contrasting approaches within European climate
1219 space, *Global Ecol. Biogeog.*, 10, 621-637, 2001.
- 1220 Smith, B., Wårlind, D., Arneth, A., Hickler, T., Leadley, P., Siltberg, J. et al.: Implications of
1221 incorporating N cycling and N limitations on primary production in an individual-based
1222 dynamic vegetation model, *Biogeosciences*, 11, 2027-2054, 2014.
- 1223 Spasojevic, M.J., Bahlai, C.A., Bradley, B.A., Butterfield, B.J., Tuanmu, M.-N., Sistla, S. et al.:
1224 Scaling up the diversity–resilience relationship with trait databases and remote sensing data:
1225 the recovery of productivity after wildfire, *Glob. Change Biol.*, 22, 1421-1432, 2016.
- 1226 Sperry, J.S., Hacke, U.G., Oren, R. & Comstock, J.P.: Water deficits and hydraulic limits to leaf
1227 water supply, *Plant, Cell & Environ.*, 25, 251-263, 2002.
- 1228 Sperry, J.S. & Love, D.M.: What plant hydraulics can tell us about responses to climate-change
1229 droughts, *New Phytol.*, 207, 14-27, 2015.
- 1230 Sperry, J.S., Wang, Y., Wolfe, B.T., Mackay, D.S., Anderegg, W.R.L., McDowell, N.G. et al.:
1231 Pragmatic hydraulic theory predicts stomatal responses to climatic water deficits, *New*
1232 *Phytol.*, 212, 577-589, 2016.
- 1233 Stovall, A.E.L., Shugart, H. & Yang, X.: Tree height explains mortality risk during an intense
1234 drought, *Nature Communications*, 10, 4385, 2019.
- 1235 Tague, C.L. & Moritz, M.A.: Plant Accessible Water Storage Capacity and Tree-Scale Root
1236 Interactions Determine How Forest Density Reductions Alter Forest Water Use and
1237 Productivity, *Front. Forests and Global Change*, 2, 2019.
- 1238 Tomasella M, Petrusa E, Petruzzellis F, Nardini A, Casolo V.: The Possible Role of Non-
1239 Structural Carbohydrates in the Regulation of Tree Hydraulics, *International Journal of*
1240 *Molecular Sciences*, 21:144, <https://doi.org/10.3390/ijms21010144>, 2020.
- 1241 Trugman, A.T., Detto, M., Bartlett, M.K., Medvigy, D., Anderegg, W.R.L., Schwalm, C. et al.:
1242 Tree carbon allocation explains forest drought-kill and recovery patterns, *Ecol. Lett.*, 21,
1243 1552-1560, 2018.
- 1244 Uriarte, M., Lasky, J.R., Boukili, V.K. & Chazdon, R.L.: A trait-mediated, neighbourhood
1245 approach to quantify climate impacts on successional dynamics of tropical rainforests,
1246 *Funct. Ecol.*, 30, 157-167, 2016.
- 1247 Vargas G., G., Brodrribb, T.J., Dupuy, J.M., González-M., R., Hulshof, C.M., Medvigy, D.,
1248 Allerton, T.A.P., Pizano, C., Salgado-Negret, B., Schwartz, N.B., Van Bloem, S.J., Waring,



- 1249 B.G. and Powers, J.S.: Beyond leaf habit: generalities in plant function across 97 tropical
1250 dry forest tree species, *New Phytol.*, 232: 148-161. <https://doi.org/10.1111/nph.17584>, 2021.
- 1251 Venturas, M. D., Todd, H. N., Trugman, A. T., & Anderegg, W. R.: Understanding and predicting
1252 forest mortality in the western United States using long-term forest inventory data and
1253 modeled hydraulic damage, *New Phytol.*, 230, 1896-1910, 2021.
- 1254 Wang, D., Heckathorn, S.A., Wang, X. & Philpott, S.M.: A meta-analysis of plant physiological
1255 and growth responses to temperature and elevated CO₂, *Oecologia*, 169, 1-13, 2012.
- 1256 Weng, E.S., Malyshev, S., Lichstein, J.W., Farrior, C.E., Dybzinski, R., Zhang, T. et al.: Scaling
1257 from individual trees to forests in an Earth system modeling framework using a
1258 mathematically tractable model of height-structured competition, *Biogeosciences*, 12, 2655-
1259 2694, 2015.
- 1260 Williams, A.P., Allen, C.D., Macalady, A.K., Griffin, D., Woodhouse, C.A., Meko, D.M. et al.:
1261 Temperature as a potent driver of regional forest drought stress and tree mortality, *Nature*
1262 *Climate Change*, 3, 292, 2012.
- 1263 Williams, A.P., Seager, R., Berkelhammer, M., Macalady, A.K., Crimmins, M.A., Swetnam,
1264 T.W. et al.: Causes and Implications of Extreme Atmospheric Moisture Demand during the
1265 Record-Breaking 2011 Wildfire Season in the Southwestern United States, *J. Applied*
1266 *Meteorology and Climatology*, 53, 2671-2684, 2014.
- 1267 Williams, L.J., Bunyavejchewin, S. & Baker, P.J.: Deciduousness in a seasonal tropical forest in
1268 western Thailand: interannual and intraspecific variation in timing, duration and
1269 environmental cues, *Oecologia*, 155, 571-582, 2008.
- 1270 Wullschleger, S.D., Hanson, P.J. & Todd, D.E.: Transpiration from a multi-species deciduous
1271 forest as estimated by xylem sap flow techniques, *For. Ecol. and Manage.*, 143, 205-213,
1272 2001.
- 1273 Xu, X., Medvigy, D., Powers, J.S., Becknell, J.M. & Guan, K.: Diversity in plant hydraulic traits
1274 explains seasonal and inter-annual variations of vegetation dynamics in seasonally dry
1275 tropical forests, *New Phytol.*, 212, 80-95, 2016.
- 1276 Yang, Y., Hillebrand, H., Lagisz, M., Cleasby, I., & Nakagawa, S.: Low statistical power and
1277 overestimated anthropogenic impacts, exacerbated by publication bias, dominate field
1278 studies in global change biology. *Glob. Change Biol.*, 28, 969– 989,
1279 <https://doi.org/10.1111/gcb.15972>, 2022.
- 1280 Zhu, K., Chiariello, N.R., Tobeck, T., Fukami, T. & Field, C.B.: Nonlinear, interacting responses
1281 to climate limit grassland production under global change, *PNAS*, 113, 10589-10594, 2016.
- 1282 Zhu, Q., Riley, W.J., Tang, J., Collier, N., Hoffman, F.M., Yang, X. et al.: Representing Nitrogen,
1283 Phosphorus, and Carbon Interactions in the E3SM Land Model: Development and Global
1284 Benchmarking, 11, 2238-2258, 2019.
- 1285 Zscheischler, J., Mahecha, M.D., von Buttlar, J., Harmeling, S., Jung, M., Rammig, A. et al.: A
1286 few extreme events dominate global interannual variability in gross primary production,
1287 *Environ. Res. Lett.*, 9, 035001, 2014.